

## ViralVectors: Compact and Scalable Alignment-free Virome Feature Generation

Sarwan Ali · Prakash Chourasia · Zahra Tayebi · Babatunde Bello · Murray Patterson

Received: date / Accepted: date

**Abstract** The amount of sequencing data for SARS-CoV-2 is several orders of magnitude larger than any virus. This will continue to grow geometrically for SARS-CoV-2, and other viruses, as many countries heavily finance genomic surveillance efforts. Hence, we need methods for processing large amounts of sequence data to allow for effective yet timely decision-making. Such data will come from heterogeneous sources: aligned, unaligned, or even unassembled raw nucleotide or amino acid sequencing reads pertaining to the whole genome or regions (e.g., spike) of interest. In this work, we propose *ViralVectors*, a compact feature vector generation from virome sequencing data that allows effective downstream analysis. Such generation is based on *minimizers*, a type of lightweight “signature” of a sequence, used traditionally in assembly and read mapping — to our knowledge, the first use minimizers in this way. We validate our approach on different types of sequencing data: (a) 2.5M SARS-CoV-2 spike sequences (to show scalability); (b) 3K Coronaviridae spike sequences (to show robustness to more genomic variability); and (c) 4K raw WGS reads sets taken from nasal-swab PCR tests (to show the ability to

---

Sarwan Ali  
Georgia State University, Atlanta, Georgia, USA  
E-mail: sali85@student.gsu.edu

Prakash Chourasia  
Georgia State University, Atlanta, Georgia, USA  
E-mail: pchourasia1@student.gsu.edu

Zahra Tayebi  
Georgia State University, Atlanta, Georgia, USA  
E-mail: ztayebi1@student.gsu.edu

Babatunde Bello  
Georgia State University, Atlanta, Georgia, USA  
E-mail: bbello1@student.gsu.edu

Murray Patterson  
Georgia State University, Atlanta, Georgia, USA  
E-mail: mpatterson30@gsu.edu

process unassembled reads). Our results show that ViralVectors outperforms current benchmarks in most classification and clustering tasks.

## 1 Introduction

The concept of *genomic surveillance* has existed for at least a decade [21], however the ongoing COVID-19 pandemic has made this an almost household term. Because such a pandemic became global at a time when sequencing technologies are quickly advancing [55], the number of SARS-CoV-2 viral genomes (viromes) available on public databases such as GISAID [22] is orders of magnitude greater than any sequenced virus in history. Not only are such volumes of data posing problems for the current algorithms used to determine the dynamics of a virus from sequencing information (*e.g.*, [23]), many countries have committed extensive budgets to vastly increase sequencing infrastructure for genomic surveillance efforts due to the pandemic. This means that the number of virome (and other molecular) sequences available in the near future will be again orders of magnitude greater than the current number of SARS-CoV-2 sequences. This inundation of sequencing data will be mostly in the form of raw sequencing reads from heterogeneous short and long-read sequencing technologies because even mapping and assembly pipelines will be overwhelmed by its sheer amount.

For this, we will need ways to swiftly extract meaningful information from sequencing data for decision-making. Furthermore, such approaches will need to be scalable to huge numbers of sequences — the number of SARS-CoV-2 sequences already accessible is already in the millions [22]. These technologies will have to be both specific and sensitive enough to detect a wide range of viruses [37]. Finally, such approaches must be able to extract such information efficiently from a variety of heterogeneous genomic or proteomic data sources with varying levels of refinement, ranging from multiply aligned consensus sequences to raw unassembled sequencing reads [52]. In this work, we offer a solution to such a problem in the form of a method we call *ViralVectors*, which generates a compact and scalable feature vector representation of viral genome (virome) data, which can be sourced from aligned, unaligned, or unassembled raw sequencing reads. Such a representation captures the necessary information from the virome yet is lightweight enough to allow quick extraction, and fast performance of downstream machine learning techniques, such as classification and clustering. We show that such a method obtains accuracy and speeds which are comparable to current benchmarks on a variety of different datasets, including: (a) a dataset of 2.5 million consensus SARS-CoV-2 spike protein sequences to demonstrate its scalability to millions of sequences; (b) a set of 3.3 thousand spike protein sequences from different genera and species of the Coronaviridae family to demonstrate its robustness in the presence of a larger degree of genomic variability; and (c) a set of raw whole-genome sequencing reads sets from the samples of a nasal-swab PCR

test of 4.3 thousand different COVID-19 patients, to demonstrate its ability to process even unassembled raw sequencing reads.

The key concept that allows us to have such a compact and scalable feature vector generation is that of a *minimizer* [41], a form of lightweight “signature” of a sequence, which is obtained by sampling the sequence. The notion of minimizer is close to that of a  $k$ -mer [14], but it is even more lightweight — minimizers are sampled from the  $k$ -mers, in fact (see Figure 1). More formally, given a sequence, the first step is to take  $k$ -mers (substrings) of length  $k$  (*i.e.*,  $k$ -mers). Then an  $m$ -mer is extracted from each  $k$ -mer (where  $m < k$ ), where the  $m$ -mer is lexicographically minimum in both forward and reverse sorted order of the  $k$ -mers. Minimizers, similarly to  $k$ -mers, have had a history of success in the domain of *de novo* assembly [18], and even read mapping [31], with the “seed-and-extend” approach — it has even had success in quickly counting  $k$ -mers [43]. In this work, we use these “seeds” directly in designing a compact feature vector representation from the minimizers, which is then used as input to typical machine learning algorithms for classification and clustering purposes.

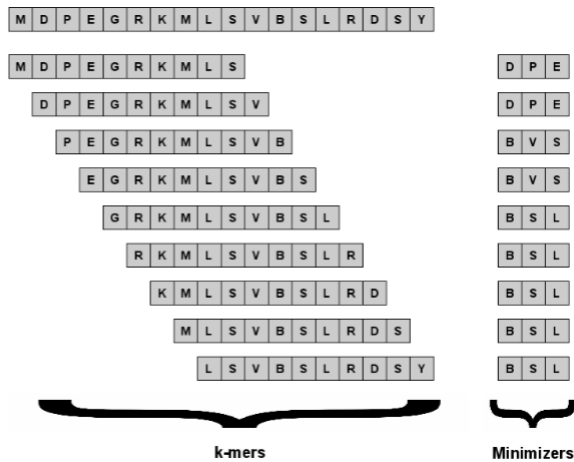


Fig. 1: Example of  $k$ -mers ( $k = 10$ ) and minimizers ( $m = 3$ ) of the amino acid sequence “MDPEGRKMLSVBSLRDSY”. For a given  $k$ -mer, its minimizer is the  $m$ -mer that is lexicographically minimum among forward and reverse (sorted) order of all  $m$ -mers within this  $k$ -mer.

Some effort has been made in the literature to classify and cluster biological sequences [1, 2, 5, 8, 29, 47]. Although existing methods successfully achieve higher classification accuracy, it is unclear whether these approaches are robust and scalable on larger datasets (millions of sequences). A kernel-based approach is proposed [20] for sequence classification using  $k$ -mers. Although

their *approximate kernel* based method is fast in terms of computing the pairwise distance between two sequences, generating the gram (kernel) matrix is a memory-extensive operation. Storing an  $n \times n$  dimensional matrix (where  $n$  is the number of sequences) in memory is practically not possible with millions of sequences. A one-hot encoding-based approach is proposed, although researchers [29] successfully classify coronavirus hosts using one-hot encoding, their method is also not scalable on “Big Data” [2, 8]. In this paper, we propose ViralVectors, a compact and scalable feature vector generation method tailored to biological sequences, which can be used as input for any machine learning algorithm for classification and clustering purposes. We show that our proposed feature vector generation approach is general and can be applied to different types of biological sequences. ViralVectors is not only scalable but also achieves higher predictive performances as compared to traditional one-hot and  $k$ -mers-based feature embedding methods. Our contributions in this paper are as follows:

1. We propose an embedding approach called ViralVectors, that outperforms the baseline feature embedding methods in terms of predictive accuracy.
2. We show the scalability of ViralVectors on larger datasets by using  $\approx 2.5$  million sequences from the GISAID website.
3. We show that the models proposed in the literature to obtain feature embeddings [2, 8, 29] are not robust on these larger datasets.
4. We show that our proposed model is general and can be applied on different types of sequences.
5. We perform clustering on ViralVectors-based embedding and show that the resultant clustering is better than the traditional Pangolin tool-based clustering and traditional one-hot and  $k$ -mers based embedding methods for clustering sequences.
6. We show the effectiveness of our compact feature vector representation by performing classification and clustering algorithms on the short reads data extracted from NCBI.
7. Using t-SNE plots, we show that the ViralVectors-based embedding may preserve the overall structure of the data while storing less information than one-hot and  $k$ -mers-based embeddings.
8. We perform statistical analysis to understand the behavior of data and predictive models.

The rest of the paper is organized as follows: Section 2 contains the related work for the given research problem. Our proposed ViralVectors-based embedding is explained in detail in Section 3. Section 4 shows the dataset detail and experimental setup information. Our results are given in Section 5. The statistical analysis of the data and different feature vectors are given in Section 6. Finally, we conclude our paper in Section 7.

## 2 Related Work

There exist several machine learning approaches based on  $k$ -mers for classification and clustering [2, 8, 9, 45], as well as more classical algorithms for sequence classification [52]. There is also a rich literature of alignment-free sequence comparison techniques [4, 11–13, 37]. Finally, there have been some recent theoretical and practical developments on minimizers [33, 56]. Although these methods are proven to be useful in respective studies, it is not clear if they can be extended on larger datasets without compromising on the predictive performance of proposed models [7, 36]. Authors in [34] propose a new set of amino acid descriptors called principal components score Vectors of Hydrophobic, Steric, and Electronic properties (VHSE) to store the chemical information relating to biological activities. A position-specific scoring matrix based approach for Protein secondary structure prediction is proposed in [26], which uses two-stage neural network. Authors in [19] compare classical encoding matrices such as one-hot encoding, VHSE8, and BLOSUM62 for end-to-end learning of amino acid embeddings for different machine learning tasks.

In [45], authors used their approach primarily on HIV, but also on experiments with dengue, influenza A, hepatitis B, and hepatitis C. A similar approach that uses mismatch kernels with support vector machines is proposed in [30] for classifying protein sequences. String kernels are also commonly used for the classification of biological sequences, nucleotides, as well as amino acid sequences [49].

Among the theoretical work on minimizers [56], the relationship has tight coupling between universal hitting sets and minimizers schemes, where minimizers schemes with low density (*i.e.*, efficient schemes) correspond to universal hitting sets of small size. Local schemes are a generalization of minimizers schemes, which can be used as replacements for minimizers schemes with the possibility of being much more efficient. This suggests even further possible future improvements to our feature vector generation.

Another issue that might affect the efficiency of underlying classification and clustering algorithms is data dimensionality. A typical technique to minimize data dimensionality is feature selection and dimensionality reduction. Several methods (supervised and unsupervised) have been proposed in the literature such as ridge regression [24], lasso regression [48], and principal component analysis (PCA) [51], etc., to get the low dimensional feature vector representations. These methods not only improve the runtime of underlying classification and clustering algorithms but also improve the predictive performance of the algorithms. Authors in [2] performs clustering on SARS-CoV-2 spike sequences and show that clustering performance could be improved by using the lasso and ridge regression. However, the major problem with all these methods is that they are not scalable on larger datasets, hence they cannot be applied in real-world settings where we can have millions of sequences. Authors in [8] use an approximate kernel method for spike sequence classification. But,

since the kernel computation is memory intensive, their proposed model does not scale to more than 7000 sequences.

### 3 Proposed Approach

In this section, we discuss our proposed method, called ViralVectors, which computes minimizers from the viral genome (virome) sequences. From these minimizers, we can then generate fixed-length feature vectors.

In the literature, it has been proven that  $k$ -mers-based frequency vectors perform better than baselines such as one-hot-encoding (OHE) [2,8]. However, a major problem with the  $k$ -mers-based approach is that for long sequences, there can be a large number of  $k$ -mers that are common to all sequences [53]. Supporting such  $k$ -mers in the frequency vector does not contribute much towards the predictive capability of the downstream classification algorithms, while, at the same time, these “redundant”  $k$ -mers contribute heavily to the runtime. This is because, for each  $k$ -mer, we need to find the location (also called bin) in the frequency vector that is associated with it. This bin searching can take as much time as the length of the frequency vector in the worst case (e.g., when the bin for a  $k$ -mer is the last one in the frequency vector). Performing the bin search operation for such  $k$ -mers that are common to all (or most) of the sequences may not be an efficient approach. This hints at the need to have more compact numerical feature vector representations of the amino acids that not only preserve the quality of the downstream predictions but also reduce the runtime of this bin-searching.

ViralVectors is a compact feature vector generation that resolves some of the problems mentioned above by using the notion of *minimizer* [41]. For a given  $k$ -mer, a minimizer is an  $m$ -mer ( $m < k$ ) that is lexicographically smallest both in forward and reverse order of the  $k$ -mer. Instead of storing the  $k$ -mers themselves, ViralVectors stores the minimizers from these  $k$ -mers, as in Figure 1. Since  $m < k$ , we are ignoring most of the amino acids in the  $k$ -mers and only preserving a fraction of the  $m$ -mers, which saves time on bin searching.

See Algorithm 1 for the pseudocode of this minimizer generation. Here, it considers a sequence  $s$  and computes the first  $k$ -mer, then slides a window over that  $k$ -mer to find the set of  $m$ -mers. Next, it will compare all the  $m$ -mers in the set from the first  $k$ -mer to find the minimum lexicographical (in forward and reverse order)  $m$ -mer and will save that in the set of minimizers (else clause starting on line 15). In the next iterations when the algorithm is producing the  $m$ -mers out of each  $k$ -mers it only needs to compare the minimum  $m$ -mer from the last iteration to the last produced  $m$ -mer of each  $k$ -mer. If it was smaller than the current minimum  $m$ -mer, it will add to the minimizers set otherwise it will continue (if the clause starts on line 7). Note that this else clause starting on line 15 is invoked in two cases: (1) when the algorithm is on its first iteration ( $idx = 0$ ), and (2) when the current minimizer is at the front of the queue ( $idx = 1$ ). Because this else clause does not get called too often on

average, in the average case, the complexity of computing minimizers with this algorithm is  $O(|s|)$ , even though the worst case is  $O(k \cdot |s|)$ , as mentioned in [31]. One can verify that the minimizers of Figure 1 are produced by Algorithm 1. To compute the minimizers from long reads, we use a  $k = 9$  and an  $m = 3$  (selected using standard validation set approach [17]).

---

**Algorithm 1: Minimzer Computation**


---

```

Input: Sequence  $s$  and integers  $k$  and  $m$ 
Output: Minimizers
1 Function ComputeMinimizer( $s, k, m$ )
2   minimizers =  $\emptyset$ 
3   queue = []
4   //  $\triangleright$ maintain queue of all  $m$ -mers in current window of size  $k$ 
5   idx = 0 //  $\triangleright$ index in queue of the current minimizer
6   for  $i \leftarrow 1$  to  $|s| - k + 1$  do
7     kmer =  $s[i : i + k]$  //  $\triangleright$ current window of size  $k$ 
8     if  $idx > 1$  then
9       queue.dequeue //  $\triangleright$ discard  $m$ -mer from the front
10      mmer =  $s[i + k - m : i + k]$  //  $\triangleright$ new  $m$ -mer to add
11      idx  $\leftarrow$  idx - 1 //  $\triangleright$ shift index of current minimizer
12      mmer = min(mmer, reverse(mmer))
13      //  $\triangleright$ lexicographically smallest forward/reverse
14      queue.enqueue(mmer) //  $\triangleright$ add new  $m$ -mer to the back
15      if  $mmer < queue[idx]$  then
16        [ idx =  $k - m$  //  $\triangleright$ check/update minimizer with new  $m$ -mer
17
18    else
19      queue = [] //  $\triangleright$ reset the queue, start from scratch
20      idx = 0
21      for  $j \leftarrow 1$  to  $k - m + 1$  do
22        mmer =  $kmer[j : j + m]$  //  $\triangleright$ compute each  $m$ -mer
23        mmer = min(mmer, reverse(mmer))
24        queue.enqueue(mmer)
25        if  $mmer < queue[idx]$  then
26          [ idx =  $j$  //  $\triangleright$ keep track of (index of) current minimizer
27
28    minimizers  $\leftarrow$  minimizers  $\cup$  queue[idx] //  $\triangleright$ add current minimizer
29  return minimizers

```

---

After generating the minimizers for each sequence, we generate the numerical feature vector representation (e.g., ViralVectors) that contains the frequency/count of the minimizers within each sequence. The length of the feature vectors for the minimizer is the same as with  $k$ -mers. The pseudocode to generate the frequency vector is given in Algorithm 2.

Traditional machine learning-based models, such as Support Vector Machine (SVM) and Naive Bayes are proven to perform efficiently on smaller data [8, 29]. However, they are not very scalable on millions of sequences [2]. For this purpose, it is required to reduce the dimensions of the ViralVectors (minimizers-based feature vector) and  $k$ -mers based frequency vectors so

**Algorithm 2:** ViralVectors Computation

---

```

Input: Set  $\mathcal{M}$  of ( $m$ -mer) minimizers on alphabet  $\Sigma$ 
Output: ViralVectors based embedding  $V$ 
1 Function ComputeFrequencyVector( $\mathcal{M}, m, \Sigma$ )
2   combos = GenerateAllCombinations( $\Sigma$ )
3    $V = [0] * |\Sigma|^m$  // Total length of (zero) vector
4   for  $i \leftarrow 1$  to  $|\mathcal{M}|$  do
5      $\text{idx} = \text{combos.index}(\mathcal{M}[i])$  // Find index of  $i^{\text{th}}$  minimizer
6      $V[\text{idx}] \leftarrow V[\text{idx}] + 1$  // Increment bin by 1
7   return  $V$ 

```

---

that the overall model is scalable on “Big Data”. Traditional methods for dimensionality reduction, such as principal component analysis, ridge regression, lasso regression, etc., are very expensive in terms of runtime and are not scalable on bigger datasets. Therefore, the scalability of machine learning algorithms is a major issue that we can face in real-world scenarios.

To deal with the scalability issue, one option is to use kernel-based algorithms that compute a gram matrix (similarity matrix) which can later be used as an input for kernel-based classifiers such as SVM. However, using the exact algorithm to compute the pair-wise distance between sequences can be very expensive. To make the kernels faster, we can use the so-called kernel trick.

**Definition 1 (Kernel Trick)** It is used to generate features for an algorithm that depends on the inner product between only the pairs of input vectors. It avoids the need to map the input data (explicitly) to a high-dimensional feature space.

The Kernel Trick depends on the following statement: *Any positive definite function  $f(x, y)$ , where  $x, y \in \mathcal{R}^d$ , defines a lifting  $\phi$  and an inner product. This is done to quickly compute the inner product between the lifted data points [40].* More formally:  $\langle \phi(x), \phi(y) \rangle = f(x, y)$ . The major problem with the kernel approach is that in the case of large training data, it suffers from large initial computational and storage costs. To deal with this drawback, we are using an approximate algorithm called Random Fourier Features (RFF) [40] in this paper. The RFF maps the input data to a low-dimensional (randomized) feature space (Euclidean inner product space). More formally:  $a : \mathcal{R}^d \rightarrow \mathcal{R}^D$ . In this way, we approximate the inner product between a pair of transformed points. More formally:

$$f(x, y) = \langle \phi(x), \phi(y) \rangle \approx a(x)'a(y) \quad (1)$$

In Equation (1),  $a$  is the low dimensional representation (unlike the lifting  $\phi$ ). In this way, we can transform the original feature vectors with  $a$  that acts as the approximate low-dimensional representation for the original feature vector. This low-dimensional feature embedding can be used as an input for classification, clustering, and regression tasks. Note that we apply RFF on both  $k$ -mers and ViralVectors-based embeddings to make them scalable for multi-million

sequences data. The dimensions of the approximate representation (from RFF) are taken as 500 (decided using standard validation set approach [17]).

## 4 Experimental Setup

In this section, we first discuss the datasets that we are using in the experiments. After that, we discuss the classification and clustering algorithms used in the experiments. In the end, we give detail about the evaluation metrics for each algorithm. All experiments are conducted using an Intel(R) Xeon(R) CPU E7-4850 v4 @ 2.10GHz having Ubuntu 64 bit OS (16.04.7 LTS Xenial Xerus) with 3023 GB memory. Implementation of ViralVectors, Spike2Vec, and OHE is done in Python. For the classification algorithms, we use 10% data for training and 90% for testing [8]. The purpose of using a smaller training dataset is to evaluate the performance gain we can achieve while using minimal data for training. From the 90% testing set, we use 10% as a validation set (for hyperparameters tuning) while 80% as a held-out testing set. All the hyperparameters, including  $k$  and  $m$ , are tuned using this 10% validation set. This training and testing set splitting process is repeated 5 times, and we then report average results.

### 4.1 Dataset Statistics

In this paper, we use three different datasets. The first dataset that we are using is a set of the full-length consensus spike protein (amino-acid) sequences from GISAID [6], which is the largest known database of SARS-CoV-2 sequences. In this data, we are using the spike protein sequences of COVID-19 viral samples from all around the world (see Figure 2c). We collected a total 2,519,386 spike protein sequences having 1327 variants in total. Figure 2c contains the distribution of the well-represented (22) COVID-19 variants in our GISAID dataset, which comprised 1,995,195 sequences (after preprocessing) in total (out of  $\approx 2.5$  million sequences).

The second data source that we are using is retrieved from the NIAD Virus Pathogen Database and Analysis Resource (ViPR) [3,39], which contains full-length spike protein sequences of different genera and species under the Coronaviridae family, and the goal is to predict which host it is most likely to affect (humans, bats, camels, etc.) — something which can be done fairly reliably using the spike sequence alone [3,29]. The distribution of the affected hosts of this ViPR dataset is given in Figure 2a.

The third data source that we are using is a collection of raw whole-genome sequencing reads sets from nasal-swab PCR tests of COVID-19-infected humans, which are collected from the NCBI website <sup>1</sup>. We collected 4,387 such sets of reads in total. The distribution of the variants (on a per-sample basis) in the NCBI short reads sets are given in Figure 2b. Note, that for this last

<sup>1</sup> <https://www.ncbi.nlm.nih.gov/>

dataset, in order to assign a variant label to each sample (the first two sets of sequences have variants identified), we needed to align the corresponding set of reads to the reference genome and call the state-of-the-art Pango tool [38]. Note, however, that since ViralVectors is an alignment-free approach, we obtain a fixed-length feature vector directly from the reads themselves.

The SARS-CoV-2 reference genome sequence (INSDC accession number GCA\_009858895.3, sequence MN9089047) used in this study was obtained from the Ensemble COVID-19 browser database [25]. It is a complete genome of 29903 bps, a reference assembly of the viral RNA genome isolates of the first cases in Wuhan-HU-1, China [54] and has been reportedly used as the standard reference widely [16].

## 4.2 Data Visualization

To see if there is any natural clustering in the data, we computed the 2D representation of the feature vectors using the t-distributed stochastic neighbor embedding (t-SNE) approach [50] and plot the 2D numerical data using scatter plots. The t-SNE plots for the ViPR dataset are given in Figure 3. We can observe that most of the hosts formed separate (sometimes multiple) clusters. This means that ViPR data are well separated. Another important point to note here is that in the case of ViralVectors (minimizer-based frequency vectors), the overall structure of the data remains the same while using only a fraction of information as compared to OHE. Note that the time complexity of t-SNE is  $O(n^2)$ . Therefore, it cannot be applied easily on 2.5 million GISAID sequences.

## 4.3 Classification and Clustering Algorithms

After generating the numerical feature vector representation, the next step is to evaluate the quality of those feature vectors. For this purpose, we use different classification and clustering algorithms.

For the classification tasks, we use different machine learning (ML) algorithms. We use Naive Bayes (NB), Logistic Regression (LR), Ridge Classifier (RC), Multi-layer Perceptron (MLP), K-Nearest Neighbors (KNN) “with  $k = 5$ , which is decided using standard validation set approach [17]”, Random Forest (RF), Logistic Regression (LR), and Decision Tree (DT).

We also use a model with a sequential constructor that is part of the Keras package (also called Keras classifier). It contains a fully connected network with 1 hidden layer with a number of neurons equal to the length of the feature vector. The activation function for input layers is “rectifier” while we use the “softmax” activation function for the output layers. We also use the efficient Adam gradient descent optimization approach with “sparse categorical cross entropy” loss function because we are dealing with multi-class classification problems. It computes the cross entropy loss between the labels and predictions. The batch size for the experiments is 100 while the number of epochs is

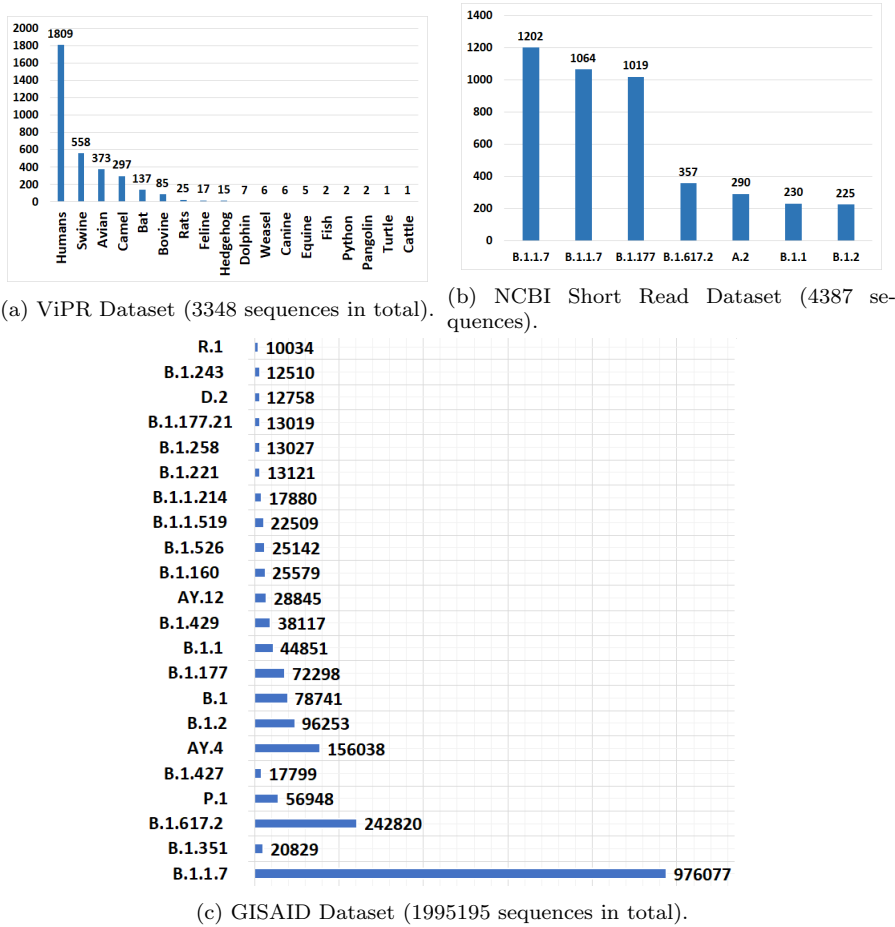


Fig. 2: (a) Host distribution in the ViPR dataset, (b) Variant distribution in the NCBI short read dataset, and (c) Variants distribution in the GISAID dataset.

taken as 10 for the training of our DL model. Note that we are using “sparse categorical cross entropy” rather than simple “categorical cross entropy” because we are using integer labels rather than the one-hot representation of labels.

For clustering analysis, the goal is to group the data into subgroups that share some degree of similarity. For clustering purposes, we are using the  $k$ -means algorithm. We used the Elbow method to select the optimum number of clusters for the  $k$ -means [2]. This method for the different numbers of clusters (ranging from 2 to 100) is performing clustering to see the trade-off between the runtime and the sum of squared error (distortion score). For the GISAID data, we take 22 as an optimal number of clusters. For the ViPR data, we use

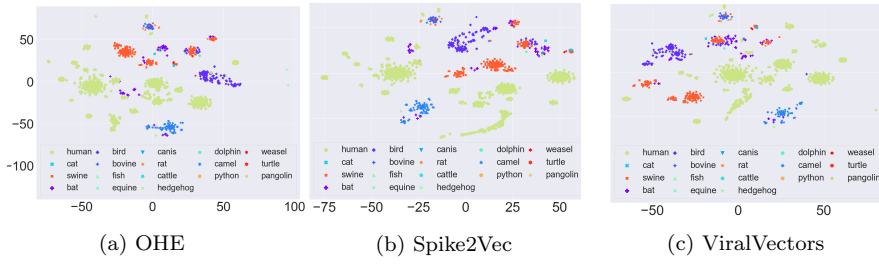


Fig. 3: t-SNE plots for ViPR dataset using (a) OHE, (b) Spike2Vec, and (c) ViralVectors.

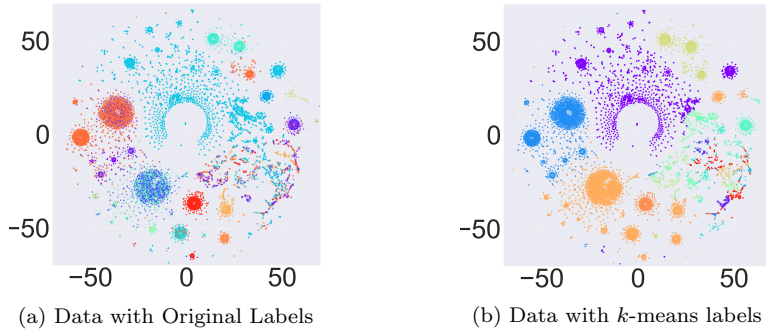


Fig. 4: t-SNE plots for the GISAID data drawn using ViralVectors with (a) original variants as labels, and (b) labels from  $k$ -means.

18 as an optimal number of clusters. Similarly, for the NCBI short-reads data, we use 7 as the optimal number of clusters.

#### 4.4 Evaluation Metrics

To evaluate the performance of ViralVectors, we perform classification and clustering. We report average accuracy, precision, recall, weighted F1, macro F1, and ROC-AUC. For metrics designed for binary classification, we apply the one-vs-rest approach to use them for multi-class classification. We also show the runtime of different classification algorithms. We ran experiments 5 times for the classification task and reported average results. To evaluate the clustering method, we use F1 (weighted), Silhouette Coefficient [42], Calinski-Harabasz Score [10], and Davies-Bouldin Score [15].

1. The Silhouette Coefficient refers to an approach that is used for the validation and interpretation of consistency within clusters of a given data. Its value range from  $-1$  to  $1$  while  $1$  is best and  $-1$  is worst clustering.
2. The Calinski-Harabasz Score is the ratio between the within-cluster dispersion and the between-cluster dispersion (a higher score is better).

3. The Davies-Bouldin Score computes the average similarity between clusters. In this metric, the similarity is a measure, which compares the distance between clusters with the size of the clusters themselves (a lower score is better in this case, as it means that clusters are well separated from each other).

#### 4.5 Baseline Models

We use different baseline and recent state-of-the-art (SOTA) methods (designed for SARS-CoV-2 sequences) to compare the results with ViralVectors. The baseline model that we are using is One Hot Embedding (OHE) [29] while the recent SOTA methods are Spike2Vec [6], PWM2Vec [3], and Pango Tool [38].

##### 4.5.1 One Hot Embedding (OHE) [29]

Since most machine learning methods do not work with biological sequence-based feature vectors, it is important to convert them into a numerical representation. A traditional method to convert sequential information into numerical representation is called one-hot embedding [8, 29]. Given a finite set of symbols in a sequence (*e.g.*, spike sequence), we call this set as an alphabet, denoted by  $\Sigma$ . In the GISAID amino acid sequences, for example, we have 21 unique characters "ACDEFGHIKLMNPQRSTVWXY" (*i.e.*, amino acids). To design a fixed-length feature vector representation, we generate a length of 21 binary vector for each amino acid, which contains a value of 1 for the position of that specific character and zero everywhere else. In the end, we concatenate all these vectors to get a final feature vector representation for a given sequence. In GISAID amino acid sequences, since the length of each spike amino acid sequence is 1273, the length of each OHE-based vector is  $1273 \times 21 = 26,733$  (more detail on the dataset can be found in Section 4.1). For the ViPR data, since the length of each spike amino acid sequence (after alignment) is 3498 (and the length of unique characters is 24), therefore, the length of the OHE vector is  $3498 \times 24 = 83,952$ . In the case of NCBI raw short reads sequencing data, the OHE does not apply, since we have variable-length unmapped reads rather than a single fixed-length sequence. After generating the feature vectors, we can give these vectors as input to machine learning algorithms for classification and clustering purposes.

*Remark 1* Note that one problem with OHE is that it required all sequences in a data to be of fixed-length [2, 8].

##### 4.5.2 Spike2Vec [6]

Since OHE does not work with variable-length sequences, a popular alignment-free method is using  $k$ -mers to preserve the order of amino acids and then

generating a fixed-length feature vector that contains the frequency of each  $k$ -mer in a virome sequence. In this setting, the first step is to compute the substrings (called mers) of length  $k$ , where  $k$  is the user-defined parameter. The  $k$ -mers are generated using a sliding window approach with the increment of 1 (see Figure 1). The total number of possible  $k$ -mers that can be generated from a virome sequence is “ $N - k + 1$ ”, where  $N$  is the length of the sequence.

**Fixed-length Representation:** Since each virome sequence can have a different number of  $k$ -mers, it is important to generate fixed-length numerical representation so that classification and clustering algorithms could be applied. For this purpose, we design a feature vector of length  $|\Sigma|^k$  (where  $\Sigma$  is the alphabet and  $k$  is user-defined parameter for  $k$ -mers) that contains the frequency/count of each  $k$ -mer within a sequence. In this paper, we are taking  $k = 3$  for all experiments unless specifically mentioned otherwise (decided using standard validation set approach [17]). In the GISAID dataset, since the total number of alphabets is 21, the length of the Spike2Vec-based feature vector is  $21^3 = 9261$ . For the ViPR-dataset, the length of the Spike2Vec-based vector is  $25^3 = 15625$ , and for NCBI short reads data, the length of Spike2Vec-based vector is  $24^3 = 13842$ .

#### 4.5.3 PWM2Vec [3]

When using a Spike2Vec method, the frequency vectors obtained are comparatively low dimension but still are high dimensional. Moreover, while generating the frequency vectors, matching the  $k$ -mers to the appropriate location/bin in the vector (bin matching) can be computationally expensive. To solve these issues, PWM2Vec [3] can be used. It is a recently proposed method for producing a fixed-length numerical feature vector based using the well-known position-weight matrix notion [46]. PWM2Vec creates a PWM from the sequence’s  $k$ -mers, and the final feature vector contains the score of each  $k$ -mer in the PWM. This enables the method to use  $k$ -mers ability to collect localization information while also capturing the significance of each amino acid’s position in the sequence (information that is lost in computing  $k$ -mer frequency vector). By combining these pieces of data in this way, a compact and broad feature embedding can be created that can be used for a variety of downstream machine-learning tasks.

#### 4.5.4 Pango Tool [38]

For clustering purposes, we also use the state-of-the-art clustering benchmark called Pango tool [38]. Since the Pango tool takes multiply aligned sequences as input, we needed to align each read set to the reference genome, call (genomic) variants, and introduce these variants into the reference sequence to generate a consensus sequence that represents this particular sample — the pipeline is available as a Snakefile [35] in our shared code repository above. The SARS-CoV-2 reference genome sequence (INSDC accession *GCA.009858895.3*,

sequence MN9089047) used in this study is obtained from Ensemble COVID-19 browser database, Ensemble COVID-19 [27, 28]. It is a complete genome of 29903 bps. The genome the reference assembly of the viral RNA genome Isolates of the first cases Wuhan-HU-1, China [54] and has been reportedly used as the standard reference widely [44].

## 5 Results and Discussion

In this section, we show the results for different classifications and clustering algorithms on all feature vector embedding approaches for all datasets.

### 5.1 Classification Results

We start by showing results for the classification of the GISAID dataset. Table 3 shows the results for different embedding methods and classification algorithms (naive Bayes, logistic regression, ridge classifier) on the GISAID dataset for the classification of variants. We can observe that the Keras classifier with ViralVectors-based embedding (minimizer with RFF) outperforms the other embedding methods for all evaluation metrics. However, in terms of runtime, Ridge Classifier with ViralVectors is performing better than all other methods.

To show the generalizability of our proposed feature embedding (ViralVectors), we use the same feature embeddings with countries and continents information separately as a class label and performed classification using the same experimental settings (as done in Table 3). The results for country classification and continent classification are given in Table 1 and Table 2. We can observe that in both scenarios, DL based classifier with ViralVectors-based feature embedding outperforms all other methods for all evaluation metrics. Note that we computed results for only 3 classifiers for the GISAID dataset due to the high computation cost of other classifiers, such as MLP and KNN. Since they were taking very long to compute results on this  $\approx 2.5$  million spike sequence data, we only used the classifiers that were best in terms of runtime. Table 4 shows the classification results for the ViPR dataset. Since the size of the dataset is smaller in this case, we use all the classifiers that were not able to compute results for the GISAID dataset. We can observe that ViralVectors-based embedding with logistic regression classifier outperforms the other two embedding approaches for all but one evaluation metric.

### 5.2 Clustering Results

This section shows results for the clustering of all datasets and embedding methods. We compare clustering results for NCBI short read dataset with the results computed using Pangolin clustering tool [38]. The results for  $k$ -means clustering applied to different embedding approaches are shown in Table 5.

Table 1: Country Classification Results (10% training set and 90% testing set) for 27 countries (2384646 spike sequences) in GISAID dataset. The best values are shown in bold.

| Embed. Method | ML Algo.         | Acc.        | Prec.       | Recall      | F1 weigh.   | F1 Macro    | ROC-AUC     | Train. runtime (sec.) |
|---------------|------------------|-------------|-------------|-------------|-------------|-------------|-------------|-----------------------|
| OHE           | NB               | 0.11        | 0.44        | 0.11        | 0.11        | 0.10        | 0.55        | 1308.4                |
|               | LR               | 0.40        | 0.46        | 0.40        | 0.33        | 0.15        | 0.55        | 2361.8                |
|               | RC               | 0.40        | 0.38        | 0.40        | 0.31        | 0.11        | 0.54        | 746.4                 |
|               | Keras Classifier | 0.49        | 0.53        | 0.49        | 0.43        | 0.24        | 0.6         | 28914.8               |
| Spike2Vec     | NB               | 0.13        | 0.41        | 0.13        | 0.15        | 0.10        | 0.55        | 1315.3                |
|               | LR               | 0.40        | 0.45        | 0.40        | 0.33        | 0.16        | 0.55        | 2736.8                |
|               | RC               | 0.39        | 0.37        | 0.39        | 0.31        | 0.11        | 0.54        | 779.4                 |
|               | Keras Classifier | 0.50        | 0.54        | 0.50        | 0.45        | 0.28        | 0.59        | 10383.6               |
| PWM2Vec       | NB               | 0.14        | 0.42        | 0.14        | 0.16        | 0.10        | 0.54        | 601.5                 |
|               | LR               | 0.40        | 0.46        | 0.40        | 0.34        | 0.16        | 0.56        | 860.7                 |
|               | RC               | 0.41        | 0.38        | 0.39        | 0.32        | 0.12        | 0.55        | <b>140.4</b>          |
|               | Keras Classifier | 0.50        | 0.55        | 0.50        | 0.46        | 0.29        | 0.60        | 466.8                 |
| ViralVectors  | NB               | 0.13        | 0.43        | 0.13        | 0.17        | 0.11        | 0.56        | 2683.72               |
|               | LR               | 0.43        | 0.48        | 0.41        | 0.35        | 0.17        | 0.57        | 4706.32               |
|               | RC               | 0.40        | 0.39        | 0.40        | 0.32        | 0.14        | 0.54        | 1492.79               |
|               | Keras Classifier | <b>0.51</b> | <b>0.56</b> | <b>0.51</b> | <b>0.47</b> | <b>0.31</b> | <b>0.63</b> | 13616.17              |

We can see that for the ViPR dataset, PWM2Vec is giving better clustering results in terms of all but one internal clustering evaluation metric. For the NCBI short reads data, although Pangolin is better in terms of Silhouette Coefficient (higher value is better), the ViralVectors-based feature embedding performs better in terms of Calinski-Harabasz Score (higher value is better) and Davies-Bouldin Score (a lower value is better).

We also use F1 (weighted) to further evaluate the clustering performance of  $k$ -means on the GISAID dataset. Based on the F1 score, since we do not have the ground truth clustering labels, we assign a label to every cluster based on the majority variant in that cluster. The F1 scores for the top 5 variants are shown in Table 6.

We can observe that ViralVectors-based feature embedding is showing the highest F1 score as compared to the other embedding methods. Note that the F1 score is on the lower side for all embedding methods in the case of the Beta variant. This is because of the lower proportion of the Beta variant in the dataset as given in Figure 2c. Since the number of sequences corresponding to the Beta variant as a label is fewer, the underlying clustering algorithm is unable to capture all the patterns in the sequences.

To visually evaluate the performance of  $k$ -means clustering, we compute the 2D numerical representation for a subset of GISAID data using the t-SNE algorithm. For each corresponding sequence, we color the actual variants

Table 2: Continent Classification Results (10% training set and 90% testing set) for 5 continents (2384646 spike sequences) for GISAID dataset. The best values are shown in bold.

| Embed. Method | ML Algo.         | Acc.        | Prec.       | Recall      | F1 weigh.   | F1 Macro    | ROC-AUC     | Train. runtime (sec.) |
|---------------|------------------|-------------|-------------|-------------|-------------|-------------|-------------|-----------------------|
| OHE           | NB               | 0.49        | 0.63        | 0.49        | 0.50        | 0.38        | 0.63        | 1457.2                |
|               | LR               | 0.67        | 0.66        | 0.67        | 0.64        | 0.33        | 0.58        | 1622.4                |
|               | RC               | 0.67        | 0.66        | 0.67        | 0.64        | 0.28        | 0.57        | 1329.1                |
|               | Keras Classifier | 0.75        | 0.76        | 0.75        | 0.72        | 0.47        | 0.65        | 30932.0               |
| Spike2Vec     | NB               | 0.48        | 0.63        | 0.48        | 0.49        | 0.36        | 0.63        | 970.6                 |
|               | LR               | 0.67        | 0.67        | 0.67        | 0.64        | 0.34        | 0.58        | 1141.9                |
|               | RC               | 0.67        | 0.66        | 0.67        | 0.64        | 0.29        | 0.57        | 832.3                 |
|               | Keras Classifier | 0.76        | 0.77        | 0.76        | 0.74        | 0.49        | 0.65        | 18631.7               |
| PWM2Vec       | NB               | 0.49        | 0.64        | 0.49        | 0.50        | 0.38        | 0.64        | 605.8                 |
|               | LR               | 0.67        | 0.67        | 0.67        | 0.65        | 0.35        | 0.59        | 840.7                 |
|               | RC               | 0.68        | 0.67        | 0.67        | 0.65        | 0.30        | 0.58        | <b>146.5</b>          |
|               | Keras Classifier | 0.77        | 0.78        | 0.77        | 0.75        | 0.52        | 0.69        | 480.1                 |
| ViralVectors  | NB               | 0.50        | 0.65        | 0.50        | 0.52        | 0.39        | 0.65        | 1348.59               |
|               | LR               | 0.68        | 0.68        | 0.68        | 0.66        | 0.36        | 0.60        | 1544.75               |
|               | RC               | 0.69        | 0.68        | 0.68        | 0.66        | 0.33        | 0.59        | 1167.42               |
|               | Keras Classifier | <b>0.79</b> | <b>0.79</b> | <b>0.79</b> | <b>0.76</b> | <b>0.56</b> | <b>0.74</b> | 13002.09              |

(true labels) for that sequence in Figure 4 (a) and compare it with the labels obtained after applying  $k$ -means clustering (on the same 2D t-SNE based representation) in Figure 4 (b). We can observe that with the  $k$ -means, most of the variants are forming separate clusters. One interesting insight is that some variants form more than one cluster. This means that they may be going away from that original variant and developing a new variant, which may be at some initial stage.

We also show the contingency tables for all datasets and embedding methods after applying  $k$ -means. The contingency tables for the GISAID data are shown in Table 7, Table 8, Table 9 for OHE, Spike2Vec, and ViralVectors, respectively.

The contingency tables for the OHE, Spike2Vec, and ViralVectors for the ViPR data are shown in Table 10, Table 11, and Table 12 for the OHE, Spike2Vec, and ViralVectors, respectively.

The contingency tables for NCBI short read data are in Table 13, Table 14, and Table 15 for the OHE, Spike2Vec, and ViralVectors, respectively. We also performed statistical analysis of the data, which involves computing information gain and SHAP analysis.

Table 3: Variants Classification Results for GISAID data (10% training and 90% testing) for top 22 variants (1995195 spike sequences). The best values are shown in bold.

| Embed. Method | ML Algo.         | Acc.        | Prec.       | Recall      | F1 weigh.   | F1 Macro    | ROC-AUC     | Train. runtime (sec.) |
|---------------|------------------|-------------|-------------|-------------|-------------|-------------|-------------|-----------------------|
| OHE [29]      | NB               | 0.30        | 0.58        | 0.30        | 0.38        | 0.18        | 0.59        | 2164.5                |
|               | LR               | 0.57        | 0.50        | 0.57        | 0.49        | 0.19        | 0.57        | 2907.5                |
|               | RC               | 0.56        | 0.48        | 0.56        | 0.48        | 0.17        | 0.56        | 1709.2                |
|               | Keras Classifier | 0.61        | 0.58        | 0.61        | 0.56        | 0.24        | 0.61        | 28971.5               |
| Spike2Vec [6] | NB               | 0.42        | 0.79        | 0.42        | 0.52        | 0.39        | 0.68        | 2056.0                |
|               | LR               | 0.68        | 0.69        | 0.68        | 0.65        | 0.49        | 0.69        | 2429.1                |
|               | RC               | 0.67        | 0.68        | 0.67        | 0.63        | 0.44        | 0.67        | 1294.2                |
|               | Keras Classifier | 0.86        | 0.87        | 0.86        | 0.83        | 0.69        | 0.83        | 13296.2               |
| PWM2Vec [3]   | NB               | 0.43        | 0.79        | 0.43        | 0.53        | 0.40        | 0.68        | 590.13                |
|               | LR               | 0.69        | 0.69        | 0.69        | 0.66        | 0.50        | 0.69        | 858.06                |
|               | RC               | 0.70        | 0.70        | 0.70        | 0.66        | 0.48        | 0.69        | <b>138.74</b>         |
|               | Keras Classifier | 0.80        | 0.78        | 0.80        | 0.78        | 0.47        | 0.74        | 460.28                |
| ViralVectors  | NB               | 0.46        | 0.81        | 0.46        | 0.55        | 0.42        | 0.71        | 2014.5                |
|               | LR               | 0.71        | 0.70        | 0.71        | 0.67        | 0.52        | 0.71        | 2328.4                |
|               | RC               | 0.71        | 0.70        | 0.71        | 0.66        | 0.49        | 0.70        | 1102.3                |
|               | Keras Classifier | <b>0.87</b> | <b>0.88</b> | <b>0.87</b> | <b>0.85</b> | <b>0.71</b> | <b>0.85</b> | 11234.1               |

Table 4: Host Classification Results on ViPR data (10% training and 90% testing) for 3348 sequences. The best values are shown in bold.

| Embed. Method | ML Algo. | Acc.        | Prec.       | Recall      | F1 weigh.   | F1 Macro    | ROC-AUC     | Train. runtime (sec.) |
|---------------|----------|-------------|-------------|-------------|-------------|-------------|-------------|-----------------------|
| OHE [29]      | NB       | 0.96        | 0.96        | 0.96        | 0.95        | 0.60        | 0.80        | 74.26                 |
|               | MLP      | 0.95        | 0.95        | 0.95        | 0.95        | 0.50        | 0.78        | 88.76                 |
|               | KNN      | 0.92        | 0.90        | 0.92        | 0.90        | 0.31        | 0.66        | 164.42                |
|               | RF       | 0.96        | 0.96        | 0.96        | 0.95        | 0.61        | 0.81        | 2.76                  |
|               | LR       | 0.96        | 0.96        | 0.95        | 0.94        | 0.62        | 0.82        | 4.80                  |
|               | DT       | 0.94        | 0.94        | 0.94        | 0.94        | 0.48        | 0.82        | 2.17                  |
| Spike2Vec [6] | NB       | 0.95        | 0.95        | 0.95        | 0.95        | 0.42        | 0.71        | 5.45                  |
|               | MLP      | 0.94        | 0.93        | 0.94        | 0.94        | 0.41        | 0.73        | 8.65                  |
|               | KNN      | 0.92        | 0.91        | 0.92        | 0.90        | 0.31        | 0.65        | 1.07                  |
|               | RF       | 0.95        | 0.94        | 0.95        | 0.95        | 0.46        | 0.72        | 0.42                  |
|               | LR       | 0.95        | 0.94        | 0.95        | 0.95        | 0.47        | 0.73        | 0.81                  |
|               | DT       | 0.93        | 0.92        | 0.93        | 0.93        | 0.38        | 0.74        | 0.26                  |
| PWM2Vec [3]   | NB       | 0.90        | 0.93        | 0.90        | 0.91        | 0.51        | 0.78        | 1.27                  |
|               | MLP      | 0.94        | 0.95        | 0.95        | 0.95        | 0.52        | 0.79        | 13.32                 |
|               | KNN      | 0.93        | 0.93        | 0.93        | 0.92        | 0.51        | 0.74        | 6.33                  |
|               | RF       | 0.93        | 0.94        | 0.94        | 0.94        | 0.63        | 0.82        | 3.09                  |
|               | LR       | 0.95        | 0.94        | 0.95        | 0.95        | 0.62        | 0.81        | 26.77                 |
|               | DT       | 0.94        | 0.95        | 0.95        | 0.95        | 0.50        | 0.81        | 1.95                  |
| ViralVectors  | NB       | 0.95        | 0.94        | 0.95        | 0.94        | 0.43        | 0.71        | 5.35                  |
|               | MLP      | 0.95        | 0.93        | 0.94        | 0.93        | 0.44        | 0.72        | 7.28                  |
|               | KNN      | 0.90        | 0.88        | 0.90        | 0.88        | 0.25        | 0.63        | 1.05                  |
|               | RF       | 0.95        | 0.95        | 0.95        | 0.95        | 0.64        | 0.82        | 0.49                  |
|               | LR       | <b>0.97</b> | <b>0.97</b> | <b>0.97</b> | <b>0.97</b> | <b>0.65</b> | <b>0.83</b> | 0.44                  |
|               | DT       | 0.95        | 0.92        | 0.92        | 0.92        | 0.38        | 0.70        | <b>0.24</b>           |

Table 5: Internal Clustering quality metrics for  $k$ -means. The best values are shown in bold.

| Dataset | Methods       | Evaluation Metrics     |                         |                      | Runtime (Sec.) |
|---------|---------------|------------------------|-------------------------|----------------------|----------------|
|         |               | Silhouette Coefficient | Calinski-Harabasz Score | Davies-Bouldin Score |                |
| ViPR    | OHE [29]      | 0.45                   | 1317.35                 | 1.37                 | 177.54         |
|         | Spike2Vec [6] | 0.63                   | <b>2517.54</b>          | 1.15                 | 36.57          |
|         | PWM2Vec [3]   | <b>0.65</b>            | 1960.95                 | <b>0.76</b>          | <b>10.05</b>   |
|         | ViralVectors  | 0.43                   | 1072.00                 | 1.32                 | 44.56          |
| NCBI    | Pangolin [38] | <b>0.64</b>            | 1702.23                 | 1.59                 | 2638.30        |
|         | Spike2Vec [6] | 0.53                   | 8402.54                 | 0.56                 | 132.13         |
|         | PWM2Vec [3]   | 0.58                   | 9812.85                 | 0.55                 | 131.52         |
|         | ViralVectors  | 0.56                   | <b>10339.07</b>         | <b>0.54</b>          | <b>130.35</b>  |

Table 6: F1 score by applying the  $k$ -means clustering algorithm on all 1327 variants (2519386 spike sequences) in the GISAID dataset. The best values are shown in bold.

| Methods       | F1 Score (Weighted) for Different Variants |              |              |              |              |
|---------------|--|--------------|--------------|--------------|--------------|
|               | Alpha                                      | Beta         | Delta        | Gamma        | Epsilon      |
| OHE [29]      | 0.041                                      | 0.041        | 0.544        | 0.643        | 0.057        |
| Spike2Vec [6] | 0.997                                      | 0.034        | 0.854        | 0.968        | 0.221        |
| PWM2Vec [3]   | 0.998                                      | 0.043        | 0.859        | 0.969        | 0.237        |
| ViralVectors  | <b>0.999</b>                               | <b>0.056</b> | <b>0.867</b> | <b>0.970</b> | <b>0.246</b> |

Table 7: Contingency tables of variants vs clusters after applying  $k$ -means on the OHE-based feature embedding on GISAID data.

| Variant    | k-means (Cluster IDs) |        |       |       |       |      |      |       |      |      |        |       |      |      |        |      |      |      |      |       |       |       |
|------------|-----------------------|--------|-------|-------|-------|------|------|-------|------|------|--------|-------|------|------|--------|------|------|------|------|-------|-------|-------|
|            | 0                     | 1      | 2     | 3     | 4     | 5    | 6    | 7     | 8    | 9    | 10     | 11    | 12   | 13   | 14     | 15   | 16   | 17   | 18   | 19    | 20    | 21    |
| AY.12      | 78                    | 1339   | 905   | 140   | 215   | 1901 | 29   | 468   | 8    | 25   | 19762  | 1153  | 260  | 4    | 1715   | 49   | 46   | 6    | 23   | 631   | 46    | 42    |
| AY.4       | 2600                  | 4480   | 27565 | 491   | 513   | 3296 | 62   | 4183  | 41   | 58   | 86178  | 7557  | 635  | 71   | 6750   | 106  | 102  | 56   | 38   | 11014 | 144   | 98    |
| B.1        | 445                   | 2033   | 61    | 32289 | 146   | 73   | 19   | 50    | 536  | 204  | 37894  | 71    | 512  | 717  | 2489   | 12   | 241  | 301  | 372  | 59    | 129   | 78    |
| B.1.1      | 577                   | 1608   | 30    | 17195 | 99    | 22   | 13   | 31    | 517  | 89   | 21182  | 39    | 409  | 771  | 1387   | 3    | 77   | 553  | 112  | 17    | 72    | 48    |
| B.1.1.214  | 2535                  | 326    | 9     | 8497  | 22    | 7    | 2    | 5     | 5    | 1    | 5987   | 8     | 60   | 11   | 379    | 0    | 9    | 1    | 2    | 5     | 5     | 4     |
| B.1.1.519  | 177                   | 2067   | 10    | 1314  | 354   | 21   | 27   | 47    | 101  | 3110 | 11903  | 45    | 203  | 68   | 1523   | 6    | 346  | 8    | 684  | 13    | 405   | 77    |
| B.1.1.7    | 3434                  | 406190 | 5653  | 8124  | 8764  | 1314 | 8154 | 13642 | 2664 | 2485 | 29611  | 4858  | 6526 | 7205 | 156188 | 240  | 8399 | 6935 | 2526 | 2376  | 11113 | 13276 |
| B.1.160    | 332                   | 2335   | 24    | 1704  | 32    | 4    | 65   | 37    | 3947 | 95   | 11696  | 10    | 917  | 2503 | 1272   | 0    | 30   | 506  | 13   | 5     | 11    | 41    |
| B.1.177    | 500                   | 9300   | 59    | 5038  | 68    | 6    | 40   | 386   | 1960 | 57   | 32072  | 27    | 1230 | 8248 | 3584   | 0    | 163  | 9355 | 20   | 24    | 21    | 140   |
| B.1.177.21 | 193                   | 1654   | 2     | 356   | 2     | 0    | 266  | 31    | 834  | 1    | 3969   | 2     | 693  | 4316 | 437    | 0    | 1    | 245  | 2    | 0     | 2     | 13    |
| B.1.2      | 2016                  | 4110   | 65    | 21920 | 503   | 55   | 16   | 109   | 294  | 1274 | 55164  | 112   | 1912 | 196  | 4246   | 1    | 733  | 75   | 2599 | 93    | 649   | 111   |
| B.1.221    | 160                   | 1482   | 11    | 606   | 25    | 2    | 29   | 26    | 959  | 20   | 5790   | 6     | 1477 | 1573 | 666    | 0    | 9    | 242  | 4    | 1     | 8     | 25    |
| B.1.243    | 1034                  | 399    | 13    | 2913  | 46    | 7    | 0    | 13    | 60   | 150  | 6652   | 13    | 131  | 14   | 522    | 0    | 104  | 5    | 329  | 18    | 74    | 13    |
| B.1.258    | 1256                  | 1763   | 9     | 690   | 17    | 5    | 31   | 59    | 471  | 9    | 5877   | 8     | 408  | 876  | 930    | 0    | 19   | 557  | 4    | 2     | 5     | 31    |
| B.1.351    | 120                   | 4918   | 93    | 300   | 287   | 58   | 24   | 107   | 139  | 77   | 11097  | 117   | 208  | 161  | 2435   | 6    | 149  | 65   | 70   | 34    | 146   | 218   |
| B.1.427    | 149                   | 1100   | 15    | 1568  | 147   | 14   | 6    | 32    | 37   | 337  | 11022  | 27    | 160  | 24   | 1089   | 3    | 193  | 1    | 1585 | 17    | 246   | 27    |
| B.1.429    | 360                   | 2651   | 22    | 3374  | 432   | 22   | 4    | 79    | 64   | 799  | 22585  | 68    | 369  | 43   | 2667   | 6    | 436  | 11   | 3513 | 21    | 505   | 86    |
| B.1.526    | 190                   | 5008   | 51    | 750   | 471   | 53   | 4    | 84    | 14   | 287  | 11414  | 117   | 318  | 20   | 2472   | 15   | 2327 | 8    | 411  | 52    | 895   | 181   |
| B.1.617.2  | 4275                  | 10938  | 48611 | 825   | 1275  | 2882 | 190  | 1351  | 78   | 121  | 124348 | 22187 | 679  | 97   | 12042  | 5048 | 266  | 38   | 136  | 6680  | 377   | 376   |
| D.2        | 2                     | 19     | 1     | 56    | 2     | 1    | 0    | 1     | 6360 | 1    | 5848   | 0     | 0    | 2    | 464    | 0    | 0    | 0    | 0    | 0     | 1     | 0     |
| P.1        | 284                   | 7037   | 284   | 784   | 11625 | 277  | 34   | 195   | 46   | 358  | 2724   | 534   | 241  | 73   | 5031   | 100  | 604  | 8    | 343  | 247   | 776   | 343   |
| R.1        | 4195                  | 1400   | 24    | 445   | 45    | 5    | 1    | 15    | 15   | 34   | 2991   | 9     | 59   | 22   | 517    | 0    | 114  | 8    | 38   | 7     | 70    | 20    |

## 6 Statistical Analysis

We use information gain (IG) to evaluate the importance of different amino acids in the prediction of class labels (hosts). The IG is defined as follows:  $IG(Class, position) = H(Class) - H(Class|position)$ . The value of  $H$  is the following:  $H = -\sum_{i \in Class} p_i \log p_i$ , where  $H$  is the entropy, and  $p_i$  is the probability of the class  $i$ . Figure 5 (d) shows the IG values (for the ViPR dataset) for different amino acids for the labels. We can observe that most of

Table 8: Contingency tables of variants vs clusters after applying k-means on the ViralVectors-based feature embedding on GISAID data.

| Variant    | k-means (Cluster IDs) |        |       |       |       |       |      |   |       |       |      |       |      |    |       |       |        |       |       |       |       |      |
|------------|-----------------------|--------|-------|-------|-------|-------|------|---|-------|-------|------|-------|------|----|-------|-------|--------|-------|-------|-------|-------|------|
|            | 0                     | 1      | 2     | 3     | 4     | 5     | 6    | 7 | 8     | 9     | 10   | 11    | 12   | 13 | 14    | 15    | 16     | 17    | 18    | 19    | 20    | 21   |
| AV.12      | 0                     | 1      | 120   | 0     | 1906  | 1288  | 1976 | 0 | 3     | 1     | 0    | 0     | 0    | 0  | 0     | 0     | 18429  | 3717  | 527   | 0     | 877   | 0    |
| AV.4       | 0                     | 4      | 26230 | 0     | 9732  | 7895  | 6630 | 0 | 317   | 6     | 0    | 0     | 0    | 0  | 0     | 0     | 88662  | 1901  | 227   | 0     | 21674 | 0    |
| R.1        | 38345                 | 1      | 0     | 0     | 2462  | 26    | 12   | 0 | 0     | 0     | 80   | 112   | 8    | 27 | 0     | 107   | 36546  | 14    | 473   | 520   | 0     | 8    |
| B.1.1      | 21373                 | 0      | 0     | 0     | 1882  | 0     | 0    | 0 | 0     | 1     | 30   | 3     | 2    | 2  | 0     | 44    | 20221  | 0     | 892   | 134   | 0     | 267  |
| B.1.1.214  | 11597                 | 0      | 0     | 0     | 2830  | 0     | 0    | 0 | 0     | 0     | 4    | 0     | 0    | 0  | 0     | 7     | 3588   | 0     | 54    | 0     | 0     | 0    |
| B.1.1.519  | 1                     | 1      | 0     | 1     | 58    | 0     | 0    | 0 | 0     | 0     | 0    | 0     | 0    | 0  | 0     | 0     | 19337  | 1     | 13    | 0     | 0     | 0    |
| B.1.1.7    | 0                     | 564607 | 0     | 18268 | 32924 | 0     | 4    | 0 | 0     | 0     | 6755 | 0     | 6600 | 0  | 18390 | 0     | 294084 | 10234 | 24211 | 0     | 0     | 0    |
| B.1.160    | 90                    | 0      | 0     | 0     | 70    | 0     | 0    | 0 | 0     | 0     | 1    | 0     | 0    | 0  | 0     | 251   | 8302   | 0     | 326   | 16677 | 0     | 0    |
| B.1.177    | 180                   | 0      | 0     | 0     | 1430  | 0     | 0    | 0 | 0     | 0     | 7    | 25865 | 0    | 0  | 0     | 12677 | 32050  | 0     | 33    | 56    | 0     | 0    |
| B.1.177.21 | 1                     | 0      | 0     | 0     | 28    | 0     | 0    | 0 | 0     | 0     | 0    | 114   | 0    | 0  | 0     | 10051 | 2825   | 0     | 0     | 0     | 0     | 0    |
| B.1.2      | 39913                 | 0      | 0     | 0     | 1961  | 2     | 0    | 0 | 0     | 0     | 52   | 0     | 0    | 3  | 0     | 198   | 46746  | 0     | 7320  | 57    | 0     | 1    |
| B.1.221    | 41                    | 0      | 0     | 0     | 84    | 0     | 0    | 0 | 0     | 0     | 8337 | 0     | 0    | 0  | 0     | 8     | 4592   | 0     | 7     | 52    | 0     | 0    |
| B.1.243    | 2140                  | 0      | 0     | 0     | 506   | 0     | 0    | 0 | 0     | 0     | 0    | 0     | 0    | 0  | 0     | 5     | 6082   | 0     | 3764  | 13    | 0     | 0    |
| B.1.258    | 1786                  | 1      | 0     | 0     | 60    | 0     | 0    | 0 | 0     | 0     | 1    | 4     | 0    | 0  | 0     | 2     | 11087  | 0     | 72    | 14    | 0     | 0    |
| B.1.351    | 0                     | 0      | 0     | 0     | 990   | 0     | 0    | 0 | 0     | 0     | 0    | 0     | 0    | 0  | 0     | 0     | 17637  | 0     | 2202  | 0     | 0     | 0    |
| B.1.427    | 7                     | 0      | 0     | 0     | 1876  | 3976  | 0    | 0 | 0     | 0     | 0    | 0     | 0    | 0  | 0     | 0     | 11900  | 0     | 40    | 0     | 0     | 0    |
| B.1.429    | 21                    | 0      | 0     | 0     | 1618  | 12884 | 0    | 0 | 0     | 0     | 0    | 0     | 0    | 1  | 0     | 0     | 22154  | 0     | 1439  | 0     | 0     | 0    |
| B.1.526    | 0                     | 0      | 0     | 0     | 1937  | 0     | 0    | 0 | 0     | 0     | 0    | 0     | 0    | 0  | 0     | 0     | 3618   | 0     | 2     | 0     | 0     | 0    |
| B.1.617.2  | 0                     | 0      | 76218 | 0     | 9693  | 98    | 1902 | 0 | 37010 | 14179 | 0    | 0     | 0    | 0  | 0     | 0     | 97629  | 316   | 4727  | 0     | 1048  | 0    |
| D.2        | 1                     | 0      | 0     | 0     | 43    | 0     | 0    | 0 | 0     | 0     | 0    | 0     | 0    | 3  | 0     | 0     | 5725   | 0     | 8     | 6978  | 0     | 0    |
| P.1        | 0                     | 0      | 0     | 0     | 67    | 0     | 0    | 0 | 0     | 0     | 0    | 0     | 0    | 0  | 0     | 0     | 25477  | 0     | 48    | 0     | 0     | 0    |
| R.1        | 0                     | 0      | 0     | 0     | 7     | 0     | 0    | 0 | 0     | 0     | 0    | 0     | 0    | 0  | 0     | 0     | 3502   | 0     | 5     | 0     | 0     | 6520 |

Table 9: Contingency tables of variants vs clusters after applying k-means on the Spike2Vec-based feature embedding on GISAID data.

| Variant    | k-means (Cluster IDs) |        |        |       |       |       |   |       |      |       |      |       |      |       |       |      |      |      |       |       |       |      |
|------------|-----------------------|--------|--------|-------|-------|-------|---|-------|------|-------|------|-------|------|-------|-------|------|------|------|-------|-------|-------|------|
|            | 0                     | 1      | 2      | 3     | 4     | 5     | 6 | 7     | 8    | 9     | 10   | 11    | 12   | 13    | 14    | 15   | 16   | 17   | 18    | 19    | 20    | 21   |
| AV.12      | 1                     | 12346  | 9340   | 114   | 4     | 0     | 0 | 809   | 0    | 0     | 0    | 0     | 1    | 0     | 0     | 947  | 0    | 3    | 0     | 0     | 1825  | 3455 |
| AV.4       | 3                     | 50380  | 49873  | 22786 | 13    | 0     | 0 | 19226 | 0    | 0     | 0    | 0     | 1    | 0     | 0     | 5735 | 3    | 243  | 0     | 0     | 6233  | 1542 |
| R.1        | 1                     | 21257  | 19814  | 0     | 163   | 35805 | 0 | 0     | 104  | 23    | 0    | 0     | 8    | 456   | 88    | 0    | 874  | 0    | 59    | 0     | 90    | 7    |
| B.1.1      | 0                     | 11519  | 12221  | 0     | 703   | 19536 | 0 | 0     | 58   | 1     | 0    | 0     | 0    | 121   | 43    | 0    | 357  | 0    | 2     | 0     | 32    | 258  |
| B.1.1.214  | 0                     | 2214   | 5340   | 0     | 1     | 10272 | 0 | 0     | 45   | 0     | 0    | 0     | 0    | 0     | 6     | 0    | 1    | 0    | 0     | 0     | 0     | 0    |
| B.1.1.519  | 1                     | 6721   | 4427   | 0     | 4     | 1     | 0 | 0     | 0    | 0     | 0    | 0     | 0    | 0     | 0     | 0    | 0    | 0    | 0     | 1     | 11353 | 0    |
| B.1.1.7    | 504917                | 204792 | 179456 | 0     | 34341 | 0     | 0 | 0     | 0    | 0     | 9751 | 16529 | 6084 | 0     | 0     | 0    | 3129 | 0    | 0     | 17074 | 4     | 0    |
| B.1.160    | 0                     | 5349   | 4328   | 0     | 25    | 83    | 0 | 0     | 0    | 0     | 0    | 0     | 0    | 15768 | 23    | 0    | 2    | 0    | 0     | 0     | 1     | 0    |
| B.1.177    | 0                     | 18422  | 16573  | 0     | 2967  | 102   | 0 | 0     | 19   | 0     | 0    | 0     | 0    | 50    | 11423 | 0    | 1    | 0    | 0     | 22736 | 0     | 6    |
| B.1.177.21 | 0                     | 1188   | 2512   | 0     | 2     | 1     | 0 | 0     | 0    | 0     | 0    | 0     | 0    | 0     | 9202  | 0    | 0    | 0    | 114   | 0     | 0     | 0    |
| B.1.2      | 0                     | 28543  | 26689  | 0     | 763   | 34770 | 0 | 0     | 4308 | 1     | 0    | 0     | 0    | 55    | 163   | 0    | 911  | 0    | 0     | 0     | 49    | 1    |
| B.1.221    | 0                     | 3201   | 2080   | 0     | 7     | 38    | 0 | 0     | 0    | 0     | 0    | 0     | 0    | 0     | 50    | 1    | 0    | 1    | 0     | 0     | 0     | 7743 |
| B.1.243    | 0                     | 3383   | 3638   | 0     | 3465  | 1973  | 0 | 0     | 6    | 0     | 0    | 0     | 0    | 13    | 5     | 0    | 27   | 0    | 0     | 0     | 0     | 0    |
| B.1.258    | 1                     | 4364   | 4557   | 0     | 4073  | 15    | 0 | 0     | 0    | 0     | 0    | 0     | 0    | 13    | 0     | 0    | 0    | 0    | 4     | 0     | 0     | 0    |
| B.1.351    | 0                     | 11436  | 9390   | 0     | 3     | 0     | 0 | 0     | 0    | 0     | 0    | 0     | 0    | 0     | 0     | 0    | 0    | 0    | 0     | 0     | 0     | 0    |
| B.1.427    | 0                     | 6740   | 7063   | 0     | 426   | 3     | 0 | 0     | 0    | 0     | 3567 | 0     | 0    | 0     | 0     | 0    | 0    | 0    | 0     | 0     | 0     | 0    |
| B.1.429    | 0                     | 13649  | 10965  | 0     | 1463  | 6     | 0 | 0     | 0    | 12034 | 0    | 0     | 0    | 0     | 0     | 0    | 0    | 0    | 0     | 0     | 0     | 0    |
| B.1.526    | 0                     | 4015   | 5436   | 0     | 3     | 0     | 0 | 0     | 19   | 0     | 0    | 0     | 0    | 0     | 0     | 0    | 1790 | 0    | 0     | 0     | 0     | 0    |
| B.1.617.2  | 0                     | 61506  | 60411  | 66632 | 5598  | 0     | 0 | 953   | 0    | 1     | 0    | 0     | 0    | 11124 | 0     | 0    | 65   | 1765 | 33167 | 0     | 1671  | 297  |
| D.2        | 0                     | 3774   | 2520   | 0     | 0     | 0     | 0 | 0     | 0    | 0     | 0    | 0     | 0    | 0     | 6460  | 0    | 1    | 0    | 0     | 0     | 3     | 0    |
| P.1        | 0                     | 15131  | 13694  | 0     | 1035  | 0     | 0 | 27088 | 0    | 0     | 0    | 0     | 0    | 0     | 0     | 0    | 0    | 0    | 0     | 0     | 0     | 0    |
| R.1        | 0                     | 2021   | 1782   | 0     | 0     | 0     | 0 | 0     | 0    | 0     | 0    | 0     | 0    | 0     | 0     | 0    | 0    | 0    | 0     | 0     | 0     | 6231 |

Table 10: Contingency tables of variants vs clusters after applying k-means on the OHE-based feature embedding on ViPR data.

| Host     | k-means (Cluster IDs) |     |   |    |   |     |   |   |   |   |    |    |    |    |      |    |    |    |     |     |   |   |
|----------|-----------------------|-----|---|----|---|-----|---|---|---|---|----|----|----|----|------|----|----|----|-----|-----|---|---|
|          | 0                     | 1   | 2 | 3  | 4 | 5   | 6 | 7 | 8 | 9 | 10 | 11 | 12 | 13 | 14   | 15 | 16 | 17 | 18  | 19  |   |   |
| bat      | 0                     | 0   | 0 | 0  | 0 | 0   | 0 | 0 | 0 | 0 | 0  | 0  | 0  | 0  | 351  | 0  | 0  | 0  | 0   | 0   | 0 | 0 |
| avian    | 0                     | 0   | 0 | 0  | 0 | 0   | 0 | 0 | 0 | 0 | 0  | 0  | 0  | 0  | 0    | 0  | 0  | 0  | 0   | 366 | 0 | 0 |
| bovine   | 0                     | 0   | 0 | 0  | 0 | 259 | 0 | 0 | 0 | 0 | 0  | 0  | 0  | 0  | 1    | 0  | 0  | 0  | 0   | 0   | 0 | 0 |
| camel    | 0                     | 154 | 0 | 0  | 0 | 0   | 0 | 0 | 0 | 0 | 0  | 0  | 0  | 0  | 1    | 0  | 0  | 0  | 0   | 0   | 0 | 0 |
| canine   | 0                     | 0   | 0 | 0  | 0 | 0   | 0 | 0 | 0 | 0 | 0  | 0  | 0  | 1  | 20   | 0  | 0  | 0  | 17  | 0   | 0 | 0 |
| feline   | 0                     | 0   | 0 | 0  | 0 | 0   | 5 | 8 | 0 | 0 | 0  | 0  | 0  | 0  | 0    | 0  | 0  | 0  | 28  | 0   | 6 | 0 |
| cattle   | 0                     | 11  | 4 | 0  | 0 | 0   | 0 | 0 | 0 | 0 | 0  | 0  | 0  | 0  | 0    | 0  | 0  | 0  | 102 | 0   | 0 | 0 |
| dolphin  | 9                     | 0   | 0 | 0  | 0 | 0   | 0 | 0 | 0 | 0 | 0  | 0  | 0  | 0  | 0    | 0  | 0  | 0  | 53  | 0   | 0 | 0 |
| equine   | 0                     | 0   | 0 | 0  | 0 | 0   | 0 | 0 | 0 | 0 | 0  | 0  | 0  | 0  | 135  | 0  | 0  | 0  | 0   | 0   | 0 | 0 |
| fish     | 57                    | 20  | 4 | 0  | 0 | 27  | 0 | 9 | 1 | 7 | 0  | 2  | 0  | 3  | 0    | 2  | 3  | 1  | 1   | 0   | 0 | 0 |
| hedgehog | 0                     | 63  | 0 | 0  | 0 | 0   | 0 | 0 | 0 | 0 | 0  | 0  | 0  | 0  | 0    | 0  | 0  | 0  | 0   | 0   | 0 | 0 |
| human    | 0                     | 0   | 5 | 0  | 0 | 0   | 0 | 0 | 0 | 0 | 0  | 0  | 0  | 0  | 0    | 0  | 0  | 0  | 3   | 0   | 0 | 0 |
| pangolin | 1                     | 0   | 0 | 0  | 0 | 0   | 0 | 0 | 0 | 0 | 0  | 0  | 0  | 0  | 1199 | 2  | 0  | 0  | 0   | 0   | 0 | 0 |
| python   | 0                     | 117 | 0 | 0  | 0 | 0   | 0 | 0 | 0 | 0 | 0  | 0  | 0  | 0  | 1    | 0  | 0  | 0  | 0   | 0   | 0 | 0 |
| rat      | 47                    | 0   | 0 | 0  | 0 | 0   | 0 | 0 | 0 | 0 | 0  | 0  | 0  | 0  | 45   | 0  | 0  | 0  | 0   | 0   | 0 | 0 |
| swine    | 0                     | 0   | 0 | 0  | 0 | 0   | 0 | 0 | 0 | 0 | 0  | 0  | 0  | 0  | 25   | 0  | 0  | 0  | 0   | 0   | 0 | 0 |
| turtle   | 23                    | 0   | 0 | 0  | 0 | 6   | 0 | 0 | 0 | 0 | 0  | 0  | 12 | 0  | 0    | 0  | 0  | 0  | 0   | 0   | 0 | 0 |
| weasel   | 0                     | 0   | 0 | 79 | 1 | 5   | 1 | 0 | 0 | 0 | 5  | 0  | 2  | 28 | 0    | 0  | 5  | 5  | 0   | 0   | 0 | 0 |

the amino acids have IG on the higher side, which means that the predictive accuracy for the machine learning models will be higher since the majority of

Table 11: Contingency tables of variants vs clusters after applying k-means on the Spike2Vec-based feature embedding on ViPR data.

| Host     | k-means (Cluster IDs) |     |   |    |   |     |   |   |   |   |    |    |    |      |    |    |    |     |    |    |
|----------|-----------------------|-----|---|----|---|-----|---|---|---|---|----|----|----|------|----|----|----|-----|----|----|
|          | 0                     | 1   | 2 | 3  | 4 | 5   | 6 | 7 | 8 | 9 | 10 | 11 | 12 | 13   | 14 | 15 | 16 | 17  | 18 | 19 |
| bat      | 0                     | 231 | 0 | 0  | 0 | 0   | 0 | 0 | 0 | 0 | 0  | 0  | 0  | 1    | 0  | 0  | 0  | 0   | 0  | 0  |
| avian    | 0                     | 0   | 0 | 0  | 0 | 0   | 0 | 0 | 0 | 0 | 0  | 0  | 0  | 25   | 0  | 0  | 0  | 0   | 0  | 0  |
| bovine   | 1                     | 0   | 0 | 0  | 0 | 0   | 0 | 0 | 0 | 0 | 0  | 0  | 0  | 1471 | 2  | 0  | 0  | 0   | 0  | 0  |
| camel    | 0                     | 0   | 0 | 79 | 1 | 5   | 1 | 0 | 0 | 0 | 5  | 0  | 3  | 48   | 0  | 0  | 22 | 5   | 0  | 0  |
| canine   | 0                     | 0   | 0 | 0  | 0 | 0   | 0 | 0 | 0 | 0 | 0  | 0  | 0  | 27   | 0  | 0  | 0  | 0   | 0  | 0  |
| feline   | 0                     | 0   | 0 | 0  | 0 | 0   | 0 | 0 | 0 | 0 | 0  | 0  | 0  | 0    | 0  | 0  | 0  | 366 | 0  | 0  |
| cattle   | 9                     | 0   | 0 | 0  | 0 | 0   | 0 | 0 | 0 | 0 | 0  | 0  | 0  | 0    | 0  | 0  | 0  | 53  | 0  | 0  |
| dolphin  | 0                     | 0   | 0 | 0  | 0 | 259 | 0 | 0 | 0 | 0 | 0  | 0  | 0  | 1    | 0  | 0  | 0  | 0   | 0  | 0  |
| equine   | 0                     | 0   | 0 | 0  | 0 | 0   | 0 | 0 | 0 | 0 | 0  | 0  | 0  | 73   | 0  | 0  | 0  | 0   | 0  | 0  |
| fish     | 90                    | 33  | 6 | 5  | 0 | 6   | 0 | 9 | 0 | 7 | 0  | 2  | 12 | 2    | 0  | 2  | 3  | 4   | 1  | 6  |
| hedgehog | 0                     | 0   | 0 | 0  | 0 | 0   | 0 | 0 | 0 | 0 | 0  | 0  | 0  | 1    | 0  | 0  | 0  | 0   | 0  | 0  |
| human    | 0                     | 0   | 0 | 0  | 0 | 0   | 0 | 0 | 0 | 0 | 0  | 0  | 0  | 79   | 0  | 0  | 0  | 0   | 0  | 0  |
| pangolin | 0                     | 0   | 0 | 0  | 0 | 0   | 5 | 8 | 0 | 0 | 0  | 0  | 0  | 0    | 0  | 0  | 0  | 28  | 0  | 0  |
| python   | 0                     | 0   | 2 | 0  | 0 | 0   | 0 | 0 | 0 | 0 | 0  | 0  | 0  | 0    | 0  | 0  | 0  | 102 | 0  | 0  |
| rat      | 0                     | 101 | 0 | 0  | 0 | 0   | 0 | 0 | 0 | 0 | 0  | 0  | 0  | 1    | 0  | 0  | 0  | 0   | 0  | 0  |
| swine    | 0                     | 0   | 0 | 0  | 0 | 0   | 0 | 0 | 0 | 0 | 0  | 0  | 0  | 34   | 0  | 0  | 0  | 0   | 0  | 0  |
| turtle   | 3                     | 0   | 0 | 0  | 0 | 27  | 0 | 0 | 1 | 0 | 0  | 0  | 0  | 1    | 0  | 0  | 0  | 0   | 0  | 0  |
| weasel   | 34                    | 0   | 0 | 0  | 0 | 0   | 0 | 0 | 0 | 0 | 0  | 0  | 0  | 45   | 0  | 0  | 0  | 0   | 0  | 0  |

Table 12: Contingency tables of variants vs clusters after applying k-means on the ViralVectors-based feature embedding on ViPR data.

| Host     | k-means (Cluster IDs) |     |   |    |   |     |   |   |   |   |    |    |    |      |    |    |    |     |    |    |
|----------|-----------------------|-----|---|----|---|-----|---|---|---|---|----|----|----|------|----|----|----|-----|----|----|
|          | 0                     | 1   | 2 | 3  | 4 | 5   | 6 | 7 | 8 | 9 | 10 | 11 | 12 | 13   | 14 | 15 | 16 | 17  | 18 | 19 |
| bat      | 0                     | 0   | 0 | 0  | 0 | 0   | 0 | 0 | 0 | 0 | 0  | 0  | 0  | 291  | 0  | 0  | 0  | 0   | 0  | 0  |
| avian    | 0                     | 0   | 0 | 0  | 0 | 0   | 0 | 0 | 0 | 0 | 0  | 0  | 0  | 139  | 0  | 0  | 0  | 0   | 0  | 0  |
| bovine   | 0                     | 0   | 0 | 0  | 0 | 0   | 0 | 0 | 0 | 0 | 0  | 0  | 0  | 0    | 0  | 0  | 0  | 237 | 0  | 0  |
| camel    | 0                     | 118 | 0 | 0  | 0 | 0   | 0 | 0 | 0 | 0 | 0  | 0  | 0  | 1    | 0  | 0  | 0  | 0   | 0  | 0  |
| canine   | 0                     | 0   | 0 | 79 | 1 | 5   | 1 | 0 | 0 | 0 | 5  | 0  | 2  | 28   | 0  | 0  | 6  | 5   | 0  | 0  |
| feline   | 0                     | 0   | 0 | 0  | 0 | 259 | 0 | 0 | 0 | 0 | 0  | 0  | 0  | 1    | 0  | 0  | 0  | 0   | 0  | 0  |
| cattle   | 0                     | 0   | 0 | 0  | 0 | 0   | 0 | 0 | 0 | 0 | 0  | 0  | 0  | 28   | 0  | 0  | 0  | 0   | 0  | 0  |
| dolphin  | 0                     | 0   | 2 | 0  | 0 | 0   | 0 | 0 | 0 | 0 | 0  | 0  | 0  | 0    | 0  | 0  | 0  | 102 | 0  | 0  |
| equine   | 1                     | 0   | 0 | 0  | 0 | 0   | 0 | 0 | 0 | 0 | 0  | 0  | 0  | 1207 | 2  | 0  | 0  | 0   | 0  | 0  |
| fish     | 0                     | 214 | 0 | 0  | 0 | 0   | 0 | 0 | 0 | 0 | 0  | 0  | 0  | 1    | 0  | 0  | 0  | 0   | 0  | 0  |
| hedgehog | 9                     | 0   | 0 | 0  | 0 | 0   | 0 | 0 | 0 | 0 | 0  | 0  | 0  | 0    | 0  | 0  | 0  | 53  | 0  | 0  |
| human    | 0                     | 0   | 0 | 0  | 0 | 0   | 4 | 8 | 0 | 0 | 0  | 0  | 0  | 0    | 0  | 0  | 0  | 28  | 0  | 0  |
| pangolin | 90                    | 33  | 6 | 5  | 0 | 6   | 1 | 9 | 0 | 7 | 0  | 2  | 13 | 2    | 0  | 2  | 19 | 4   | 1  | 6  |
| python   | 34                    | 0   | 0 | 0  | 0 | 0   | 0 | 0 | 0 | 0 | 0  | 0  | 0  | 45   | 0  | 0  | 0  | 0   | 0  | 0  |
| rat      | 0                     | 0   | 0 | 0  | 0 | 0   | 0 | 0 | 0 | 0 | 0  | 0  | 0  | 20   | 0  | 0  | 0  | 0   | 0  | 0  |
| swine    | 0                     | 0   | 0 | 0  | 0 | 0   | 0 | 0 | 0 | 0 | 0  | 0  | 0  | 45   | 0  | 0  | 0  | 0   | 0  | 0  |
| turtle   | 3                     | 0   | 0 | 0  | 0 | 27  | 0 | 0 | 1 | 0 | 0  | 0  | 0  | 1    | 0  | 0  | 0  | 0   | 0  | 0  |
| weasel   | 0                     | 0   | 0 | 0  | 0 | 0   | 0 | 0 | 0 | 0 | 0  | 0  | 0  | 0    | 0  | 0  | 0  | 129 | 0  | 0  |

the amino acids are contributing towards the prediction of class labels. This type of analysis helps us to understand the importance of different features in the data, and we can eventually ignore or remove the uninformative features from the data in order to improve the predictive performance.

## 6.1 SHAP Analysis

We also use SHAP analysis [32] to understand how significant each factor is in determining the final label prediction of the model outputs. For this purpose, SHAP analysis runs a large number of predictions and compares a variable's impact against the other features. The SHAP analysis (for the ViPR dataset)

Table 13: Contingency tables of variants vs clusters after applying k-means on the OHE-based feature embedding on NCBI short read data.

| Variant   | k-means (Cluster IDs) |     |    |     |     |     |    |
|-----------|-----------------------|-----|----|-----|-----|-----|----|
|           | 0                     | 1   | 2  | 3   | 4   | 6   | 7  |
| A.2       | 266                   | 0   | 0  | 0   | 12  | 10  | 2  |
| B.1       | 863                   | 0   | 3  | 5   | 49  | 141 | 3  |
| B.1.1     | 201                   | 0   | 0  | 1   | 16  | 12  | 0  |
| B.1.1.7   | 1                     | 699 | 76 | 301 | 9   | 40  | 76 |
| B.1.177   | 947                   | 0   | 1  | 0   | 37  | 34  | 0  |
| B.1.2     | 193                   | 0   | 1  | 0   | 8   | 22  | 1  |
| B.1.617.2 | 24                    | 0   | 3  | 0   | 317 | 13  | 0  |

Table 14: Contingency tables of variants vs clusters after applying k-means on the Spike2Vec-based feature embedding on NCBI short read data.

| Variant   | k-means (Cluster IDs) |     |    |   |     |    |   |
|-----------|-----------------------|-----|----|---|-----|----|---|
|           | 0                     | 1   | 2  | 3 | 4   | 6  | 7 |
| A.2       | 50                    | 150 | 0  | 0 | 86  | 4  | 0 |
| B.1       | 45                    | 739 | 2  | 0 | 260 | 15 | 3 |
| B.1.1     | 25                    | 126 | 0  | 1 | 73  | 2  | 3 |
| B.1.1.7   | 52                    | 596 | 1  | 0 | 547 | 6  | 0 |
| B.1.177   | 54                    | 513 | 0  | 0 | 452 | 0  | 0 |
| B.1.2     | 6                     | 167 | 0  | 0 | 51  | 1  | 0 |
| B.1.617.2 | 26                    | 141 | 31 | 0 | 114 | 45 | 0 |

Table 15: Contingency tables of variants vs clusters after applying k-means on the ViralVectors-based feature embedding on NCBI short read data.

| Variant   | k-means (Cluster IDs) |   |    |    |     |   |    |
|-----------|-----------------------|---|----|----|-----|---|----|
|           | 0                     | 1 | 2  | 3  | 4   | 6 | 7  |
| A.2       | 91                    | 0 | 14 | 0  | 185 | 0 | 0  |
| B.1       | 209                   | 0 | 23 | 0  | 827 | 2 | 3  |
| B.1.1     | 70                    | 1 | 13 | 0  | 142 | 3 | 1  |
| B.1.1.7   | 562                   | 0 | 14 | 1  | 625 | 0 | 0  |
| B.1.177   | 425                   | 0 | 7  | 0  | 587 | 0 | 0  |
| B.1.2     | 18                    | 0 | 3  | 0  | 204 | 0 | 0  |
| B.1.617.2 | 93                    | 3 | 28 | 30 | 162 | 0 | 41 |

for different feature embeddings (Spike2Vec, PWM2Vec, and ViralVectors) are given in Figure 5. Note that for OHE, we were getting memory errors because of the high dimensionality of the feature vectors, which is why we have not included the SHAP analysis figure for OHE. We can observe that for the human label, the majority of the top contributing amino acids are taking part, which shows that humans are easier to classify as compared to the other labels. For Spike2Vec and Viral Vectors, the label Bat is the second most important host;

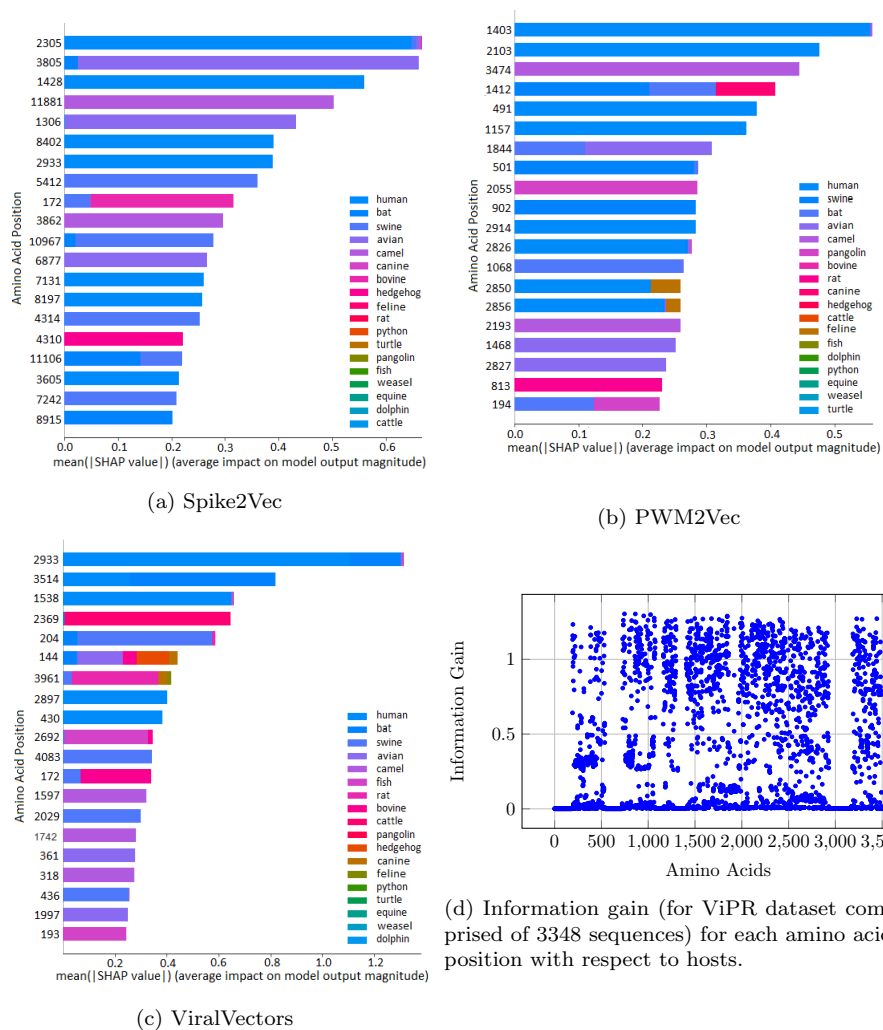


Fig. 5: SHAP Analysis (for ViPR dataset) for top amino acids using different embedding methods (a) Spike2Vec, (b) PWM2Vec, and (c) ViralVectors. Figure (d) shows Information Gain values for the ViPR dataset.

for PWM2Vec, the label Swine is the second most important host. This type of analysis can help us to decide which labels we should focus more on to increase the predictive performance of the underlying machine learning classifiers. The code for SHAP analysis is available online <sup>2</sup>.

<sup>2</sup> <https://github.com/slundberg/shap>

## 7 Conclusion

We propose an efficient, scalable, and compact feature embedding method, called ViralVectors, that can encode the sequential information of viromes into fixed-length vectors. Results for different datasets on multiple classifications and clustering algorithms show that ViralVectors is not only scalable to millions of sequences but is also, a general approach that can be applied in any setting, and outperforms the traditional methods in most cases. One possible extension for the future is to extract multiple minimizers from each short read in the case of the NCBI data and then compare it with the ViralVectors-based embedding in which we are taking just one minimizer from each short read, regardless of its size. Another possible extension is to propose an approximate algorithm to generate the frequency vector to further reduce the computational overhead.

## References

1. Ali, S.: Evaluating covid-19 sequence data using nearest-neighbors based network model. arXiv preprint arXiv:2211.10546 (2022)
2. Ali, S., Ali, T.E., Khan, M.A., Khan, I., Patterson, M.: Effective and scalable clustering of sars-cov-2 sequences. In: International Conference on Big Data Research (ICBDR), pp. 42–49 (2021)
3. Ali, S., Bello, B., Chourasia, P., Punathil, R.T., Zhou, Y., Patterson, M.: Pwm2vec: An efficient embedding approach for viral host specification from coronavirus spike sequences. *Biology* **11**(3), 418 (2022)
4. Ali, S., Bello, B., Tayebi, Z., Patterson, M.: Characterizing sars-cov-2 spike sequences based on geographical location. *Journal of Computational Biology* (2023)
5. Ali, S., Murad, T., Chourasia, P., Patterson, M.: Spike2signal: Classifying coronavirus spike sequences with deep learning. In: 2022 IEEE Eighth International Conference on Big Data Computing Service and Applications (BigDataService), pp. 81–88 (2022)
6. Ali, S., Patterson, M.: Spike2vec: An efficient and scalable embedding approach for covid-19 spike sequences. In: IEEE International Conference on Big Data (Big Data), pp. 1533–1540 (2021)
7. Ali, S., Sahoo, B., Khan, M.A., Zelikovsky, A., Khan, I.U., Patterson, M.: Efficient approximate kernel based spike sequence classification. *IEEE/ACM Transactions on Computational Biology and Bioinformatics* (2022)
8. Ali, S., Sahoo, B., Ullah, N., Zelikovskiy, A., Patterson, M., Khan, I.: A k-mer based approach for sars-cov-2 variant identification. In: International Symposium on Bioinformatics Research and Applications, pp. 153–164 (2021)
9. Ali, S., Sahoo, B., Zelikovsky, A., Chen, P.Y., Patterson, M.: Benchmarking machine learning robustness in covid-19 genome sequence classification. *Scientific Reports* **13**(1), 4154 (2023)
10. Caliński, T., Harabasz, J.: A dendrite method for cluster analysis. *Communications in Statistics-theory and Methods* **3**(1), 1–27 (1974)
11. Chourasia, P., Ali, S., Ciccolella, S., Della Vedova, G., Patterson, M.: Clustering sars-cov-2 variants from raw high-throughput sequencing reads data. In: Computational Advances in Bio and Medical Sciences: 11th International Conference, ICCABS, pp. 133–148 (2022)
12. Chourasia, P., Ali, S., Ciccolella, S., Vedova, G.D., Patterson, M.: Reads2vec: Efficient embedding of raw high-throughput sequencing reads data. *Journal of Computational Biology* (2023)
13. Chourasia, P., Murad, T., Tayebi, Z., Ali, S., Khan, I.U., Patterson, M.: Efficient classification of sars-cov-2 spike sequences using federated learning. arXiv preprint arXiv:2302.08688 (2023)

14. Compeau, P.E.C., Pevzner, P.A., Tesler, G.: How to apply de bruijn graphs to genome assembly. *Nature Biotechnology* **29**(11), 987–991 (2011)
15. Davies, D.L., Bouldin, D.W.: A cluster separation measure. *IEEE transactions on pattern analysis and machine intelligence* (2), 224–227 (1979)
16. De Silva, N.H., Bhai, J., Chakiachvili, M., Contreras-Moreira, B., Cummins, C., Frankish, A., Gall, A., Genez, T., Howe, K.L., Hunt, S.E., et al.: The ensembl covid-19 resource: Ongoing integration of public sars-cov-2 data. *bioRxiv* pp. 2020–12 (2021)
17. Devijver, P., Kittler, J.: Pattern recognition: A statistical approach. In: London, GB: Prentice-Hall, pp. 1–448 (1982)
18. Ekim, B., Berger, B., Chikhi, R.: Minimizer-space de bruijn graphs: Whole-genome assembly of long reads in min on a pc. *Cell Systems* **12**(10), 958–968.e6 (2021)
19. ElAbd, H., Bromberg, Y., Hoarfrost, A., Lenz, T., Franke, A., Wendorff, M.: Amino acid encoding for deep learning applications. *Bioinformatics* **21**(1), 1–14 (2020)
20. Farhan, M., Tariq, J., Zaman, A., Shabbir, M., Khan, I.: Efficient approx algorithms for strings kernel based sequence classification. In: *Advances in neural info processing sys (NeurIPS)*, pp. 6935–6945. . (2017)
21. Gardy, J., Loman, N.: Towards a genomics-informed, real-time, global pathogen surveillance system. *Nature Reviews Genetics* **19**, 9–20 (2018)
22. GISAID Website: <https://www.gisaid.org/>. [Online; accessed 5-Jan-2022]
23. Hadfield, J., Megill, C., Bell, S., Huddleston, J., Potter, B., Callender, C., Sagulenko, P., Bedford, T., Neher, R.: Nextstrain: real-time tracking of pathogen evo. *Bioinformatics* **34**, 4121–4123 (2018)
24. Hoerl, A.E., Kannard, R.W., Baldwin, K.F.: Ridge regression: some simulations. *Communications in Statistics-Theory and Methods* **4**(2), 105–123 (1975)
25. Howe, K.L., Contreras-Moreira, B., De Silva, N., Maslen, G., Akanni, W., Allen, J., Alvarez-Jarreta, J., Barba, M., Bolser, D.M., Cambell, L., et al.: Ensembl genomes 2020—enabling non-vertebrate genomic research. *Nucleic acids research* **48**(D1), D689–D695 (2020)
26. Jones, D.T.: Protein secondary structure prediction based on position-specific scoring matrices. *Journal of molecular biology* **292**(2), 195–202 (1999)
27. K.L., H., B., C.M., N., D.S., G., M., et al.: Ensembl genomes 2020—enabling non-vertebrate genomic research. *Nucleic. Acids. Res* **48**, D689–D695 (2020)
28. K.L., H., P., A., J., A., et al.: Ensembl 2021. *Nucleic Acids Res* **49**, D884–D891 (2021)
29. Kuzmin, K., Adeniyi, A.E., DaSouza Jr, A.K., Lim, D., Nguyen, H., Molina, N.R., Xiong, L., Weber, I.T., Harrison, R.W.: Machine learning methods accurately predict host specificity of coronaviruses based on spike sequences alone. *Biochemical and Biophysical Research Communications* **533**(3), 553–558 (2020)
30. Leslie, C.S., Eskin, E., Cohen, A., Weston, J., Noble, W.S.: Mismatch string kernels for discriminative protein classification. *Bioinformatics* **20**(4), 467–476 (2004)
31. Li, H.: Minimap and miniasm: fast mapping and de novo assembly for noisy long sequences. *Bioinformatics* **32**, 2103–2110 (2016)
32. Lundberg, S.M., Lee, S.I.: A unified approach to interpreting model predictions. In: I. Guyon, U.V. Luxburg, S. Bengio, H. Wallach, R. Fergus, S. Vishwanathan, R. Garnett (eds.) *Advances in Neural Information Processing Systems* 30, pp. 4765–4774 (2017)
33. Marçais, G., DeBlasio, D., Kingsford, C.: Asymptotically optimal minimizers schemes. *Bioinformatics* **34**, i13–i22 (2018)
34. Mei, H., Liao, Z.H., Zhou, Y., Li, S.Z.: A new set of amino acid descriptors and its application in peptide qsars. *Peptide Science: Original Research on Biomolecules* **80**(6), 775–786 (2005)
35. Mölder, F., Jab, K., Letcher, B., et al.: Sustainable data analysis with snakemake. *F1000Res* **10**(33) (2021)
36. Murad, T., Ali, S., Patterson, M.: Exploring the potential of gans in biological sequence analysis. *arXiv preprint arXiv:2303.02421* (2023)
37. Ondov, B., Treangen, T., Melsted, P., et al.: Mash: fast genome and metagenome distance estimation using minhash. *Genome Biol* **17**(132) (2016)
38. Phylogenetic Assignment of Named Global Outbreak LINeages (Pangolin): <https://cov-lineages.org/resources/pangolin.html>. [Online; accessed 4-Jan-2022]

39. Pickett, B.E., Sadat, E.L., Zhang, Y., Noronha, J.M., Squires, R.B., Hunt, V., Liu, M., Kumar, S., Zaremba, S., Gu, Z., et al.: Vipr: an open bioinformatics database and analysis resource for virology research. *Nucleic acids research* **40**(D1), D593–D598 (2012)
40. Rahimi, A., Recht, B., et al.: Random features for large-scale kernel machines. In: *NIPS*, vol. 3, p. 5 (2007)
41. Roberts, M., Haynes, W., Hunt, B., Mount, S., Yorke, J.: Reducing storage requirements for biological sequence comparison. *Bioinformatics* **20**, 3363–9 (2004)
42. Rousseeuw, P.J.: Silhouettes: a graphical aid to the interpretation and validation of cluster analysis. *Journal of computational and applied mathematics* **20**, 53–65 (1987)
43. S, D., M, K., S, G., A, D.G.: Kmc 2: fast and resource-frugal k-mer counting. *Bioinformatics* **31**(10), 1569–76 (2015)
44. Silva, N.H.D., Bhai, J., Chakiachvili, M., et al.: The ensembl covid-19 resource: ongoing integration of public sars-cov-2 data. *Nucleic Acids Research* (2021)
45. Solis-Reyes, S., Avino, M., Poon, A., Kari, L.: An open-source k-mer based machine learning tool for fast and accurate subtyping of hiv-1 genomes. *Plos One* (2018)
46. Stormo, G.D., Schneider, T.D., Gold, L., Ehrenfeucht, A.: Use of the ‘Perceptron’ algorithm to distinguish translational initiation sites in *E. coli*. *Nucleic Acids Research* **10**(9), 2997–3011 (1982)
47. Tayebi, Z., Ali, S., Patterson, M.: Robust representation and efficient feature selection allows for effective clustering of sars-cov-2 variants. *Algorithms* **14**(12), 348 (2021)
48. Tibshirani, R.: Regression shrinkage and selection via the lasso. *Journal of the Royal Statistical Society: Series B (Methodological)* **58**(1), 267–288 (1996)
49. Toussaint, N.C., Widmer, C., Kohlbacher, O., Rätsch, G.: Exploiting physico-chemical properties in string kernels. *BMC bioinformatics* **11**(8), 1–9 (2010)
50. Van D M. L. and Hinton, G.: Visualizing data using t-sne. *Journal of Machine Learning Research (JMLR)* **9**(11) (2008)
51. Wold, S., Esbensen, K., Geladi, P.: Principal component analysis. *Chemometrics and intelligent laboratory systems* **2**(1-3), 37–52 (1987)
52. Wood, D., Salzberg, S.: Kraken: ultrafast metagenomic sequence classification using exact alignments. *Genome Biol* **15** (2014)
53. Wood, D.E., Salzberg, S.L.: Kraken: ultrafast metagenomic sequence classification using exact alignments. *Genome biology* **15**(3), 1–12 (2014)
54. Wu, F., Zhao, S., Yu, B., Chen, Y.M., Wang, W., Song, Z.G., Hu, Y., Tao, Z.W., Tian, J.H., Pei, Y.Y., et al.: A new coronavirus associate with human respiratory disease. *Nature* **579**(7798), 265–269 (2020)
55. ZD, S., SY, L., F, F., RH, C., C, Z., MJ, E., et al.: Big data: Astronomical or genetical? *PLoS Biology* **13**(7), e1002195 (2015)
56. Zheng, H., Kingsford, C., Marçais, G.: Lower density selection schemes via small universal hitting sets with short remaining path len. In: *ICRCMB*, pp. 202–217. Springer (2020)



**Sarwan Ali** is a Ph.D. student at Department of Computer Science, Georgia State University working in the field of Bioinformatics, Data mining, Big data, and Machine Learning.



**Prakash Chourasia** is a Ph.D. student at Department of Computer Science, Georgia State University working in the field of Bioinformatics and Machine Learning.



**Zahra Tayebi** is a Ph.D. student at Department of Computer Science, Georgia State University working in the field of Bioinformatics and Algorithms.



**Babatunde Bello** is an MS student at Department of Computer Science, Georgia State University working in the field of Biology, Chemistry, and Bioinformatics.



**Murray Patterson** is an Assistant Professor at Georgia State University working in the fields of Bioinformatics, Computational Biology, Algorithms, and Combinatorics.